Mol. Cell. Biol. doi:10.1128/MCB.01457-14

Elongation factor 2 kinase is regulated by proline hydroxylation and protects cells during hypoxia

Claire E. J. Moore, Halina Mikolajek, Sergio Regufe da Mota, [1]Xuemin Wang, [2]Justin W. Kenney, Jörn M. Werner and *[1]Christopher G. Proud

Centre for Biological Sciences, University of Southampton, Southampton, SO17 1BJ, UK

[1] current address: South Australian Health & Medical Research Institute, PO Box 11060, Adelaide, SA5001, Australia and School of Molecular and Biomedical Sciences, University of Adelaide

[2] current address: Program in Neurosciences and Mental Health, The Hospital for Sick Children, Toronto, ON M5G 0A4, Canada

* Corresponding author: email: christopher.proud@sahmri.com

Running title: Control of eEF2 kinase by proline hydroxylation

Protein synthesis, and especially translation elongation, requires large amounts of energy, which is often generated by oxidative metabolism. Elongation is controlled by phosphorylation of eukaryotic elongation factor 2 (eEF2), which inhibits its activity and is catalysed by eEF2 kinase (eEF2K), a calcium/calmodulin-dependent α-kinase.

Hypoxia causes the activation of eEF2K and induces eEF2 phosphorylation independently of previously-known inputs into eEF2K. Here, we show that eEF2K is subject to hydroxylation on proline-98. Proline hydroxylation is catalysed by proline hydroxylases, oxygen-dependent enzymes which are inactivated during hypoxia. Pharmacological inhibition of proline hydroxylases also stimulates eEF2 phosphorylation. Pro98 lies in a universally-conserved linker between the calmodulin-binding and catalytic domains of eEF2K. Its hydroxylation partially impairs the binding of calmodulin to eEF2K and markedly limits the CaM-stimulated activity of eEF2K. Neuronal cells depend on oxygen and eEF2K helps to protect them from hypoxia.

eEF2K is the first example of a protein directly involved in a major energy-consuming process to be regulated by proline hydroxylation. Since eEF2K is cytoprotective during hypoxia and other conditions of nutrient insufficiency, it may be a valuable target for therapy of poorly-vascularised solid tumours.

Introduction:

Many cells require aerobic metabolism to generate energy, necessitating an adequate supply of oxygen. Protein synthesis is a major energy-consuming process, especially translation elongation which uses both ATP (for amino acyl-tRNA charging) and GTP (at least two are used during each round of the elongation process). Overall, at least four ATP equivalents are used for each amino acid added to the growing chain during elongation. Elongation rates can be regulated through the phosphorylation of eukaryotic elongation factor 2 (eEF2) (43). Phosphorylation of eEF2 on Thr56 by eEF2 kinase (eEF2K) inhibits its ability to interact with ribosomes (7) thereby impairing translation elongation. Indeed, a range of studies has shown that increased phosphorylation of eEF2 is associated with slower ribosomal movement along the mRNA (e.g., (27,31,39)).

eEF2K interacts with calmodulin (CaM) through a binding site which lies almost immediately N-terminal to its catalytic domain (12,37). The catalytic domain belongs to the small group of (six) mammalian α-kinases, rather than the main protein kinase superfamily; α-kinases show no sequence homology and only limited three-dimensional structural homology to other protein kinases (14,35). eEF2K activity is regulated through several signaling pathways linked, e.g., to nutrient availability; these include signaling through the mammalian target of rapamycin complex 1 (mTORC1), which represses eEF2K activity, and the AMP-activated protein kinase (AMPK), a key cellular energy sensor (20) which causes activation of eEF2K (3,22), probably in part by inhibiting mTORC1 signaling. Both inputs operate such that nutrient starvation activates eEF2K to inhibit eEF2 and slow down elongation. This, in turn, will help conserve ATP (and GTP, which are interconverted by

Molecular and Cellular Biology

nucleoside diphosphate kinase) and amino acids, key precursors for protein production. Indeed, recent studies show that eEF2K plays a key role in the ability of cancer cells to cope with nutrient starvation and that they adapt to poor nutrient availability by switching on eEF2K (likely via AMPK) (31). To date, no substrates for eEF2K other than eEF2 have been reported.

Oxygen starvation (hypoxia) also imposes a stress on many cells, e.g., by impairing ATP production by mitochondria (and other effects). Hypoxia is especially important in highly oxidative tissues such as heart muscle and brain, e.g., during cardiac ischemia or stroke. One important mechanism by which cells can respond to inadequate oxygen (hypoxia) involves the regulation of proteins by proline hydroxylation. Proline hydroxylation is catalysed by proline hydroxylases (PHDs), which require oxygen as co-substrate (24). The best-known example of control of an intracellular protein by proline hydroxylation is the transcription factor hypoxia-inducible factor (HIF)-1α. During normoxia, proline hydroxylation of HIF1α renders it a substrate for the E3 ubiquitin-ligase von Hippel-Lindau, leading to its proteasome-mediated destruction (24). Hydroxylation of HIF1α is impaired during hypoxia, allowing its stabilisation and increasing its levels. This enhances the transcription of HIF1α target genes, which encode proteins that help cells withstand hypoxia, e.g., the glucose transporter Glut1 (17). Identifying proteins that are subject to proline hydroxylation is challenging and very few other intracellular proteins are so far known to be regulated by this modification. In particular, no PHD targets that regulate energy-demanding processes have previously been discovered.

Molecular and Cellular Biology

Previous studies, in cardiomyocytes and in breast cancer cells, have shown that the phosphorylation of eEF2 increases during hypoxia and contributes to cell survival under these conditions (10,46). However, it was unclear whether eEF2K is actually activated under these conditions. More recently, it has been shown that inhibition of prolyl hydroxylases increases eEF2 phosphorylation (42), but again the mechanism remained unclear. Here we show that eEF2K is activated during hypoxia or upon inhibition of prolyl hydroxylases. We show that eEF2K is inhibited by its hydroxylation on a highly conserved proline residue, restricting its activity during normoxia. During hypoxia, when proline hydroxylation is impaired, eEF2K becomes more active to inhibit protein synthesis, thus protecting cells from hypoxia. This is the first example of direct regulation by proline hydroxylation of an enzyme involved in damping down a major energy-consuming process.

Molecular and Cellular Biology

Molecular and Cellular Biology

Materials and Methods

Antibodies and chemicals

The mTOR inhibitors, rapamycin was purchased from Calbiochem (Nottingham, UK) and AZD8055 was purchased from Tocris. FG-4497 was synthesized at FibroGen, Inc. (San Francisco, CA). Where indicated, cells were exposed to the PHD inhibitor FG-4497 at indicated concentrations for indicated periods of time. Control conditions included exposure to equivalent concentrations of vehicle. All other chemicals and biochemicals were from Sigma unless otherwise indicated. Antibodies for anti-eEF2K human and mouse which were generously provided by the Division of Signal Transduction Therapy, University of Dundee, UK. Anti-FLAG was from Sigma and the anti-phospho-eEF2(Thr56) antibody was generated by Eurogentec; all other antibodies were from Cell Signaling Technology. eEF2 for kinase assays was purified from HeLa cell cytoplasm (essentially as described in (26)).

Cell culture and treatment

Mouse embryonic fibroblasts (MEFs) from eEF2K$^{-/-}$ (knockout) mice and matched wild-type counterparts were prepared from embryos at embryonic day 13.5. MEFs from eEF2K (WT) and eEF2K$^{-/-}$ mouse embryos were cultured in Dulbecco's modified Eagle's medium (DMEM; Invitrogen) supplemented with 10% foetal calf serum (FCS), and 100 units/mL penicillin, and 0.1 mg/mL streptomycin (Invitrogen) at 37°C in a humidified atmosphere of 5% CO_2. TSC2$^{-/-}$MEFs and the corresponding TSC2$^{+/+}$ cell line were generously provided by Dr. David Kwiatkowski (Harvard University, Boston). HeLa cells were grown in DMEM (Dulbecco's modified Eagle's medium) supplemented with 10% (v/v) FBS (foetal

bovine serum), 2 mM glutamine and 1% penicillin/streptomycin. Colorectal adenocarcinoma HCT116 cells were generously provided by Janssen Pharmaceuticals and cultured using standard procedures in a 37°C humidified incubator with 5% CO_2 in high-glucose McCoy's 5A Modified Medium (Invitrogen) supplemented with 10% (v/v) foetal calf serum, 100 units/mL penicillin, and 0.1 mg/mL streptomycin. HEK (human embryonic kidney)-293 cells were cultured and transfected as described previously (19). Wild type (WT) and AMPKα1/α2 double knockout (DKO) MEFs (28) were generously provided by Dr Benoit Viollet (Institute Cochin, University of Paris). Cells were grown in DMEM (Dulbecco's modified Eagle's medium) supplemented with 10% (v/v) fetal bovine serum, 2 mM glutamine and 1% penicillin/streptomycin.

Human lung carcinoma A549 cell line containing an IPTG-inducible shRNA plasmid directed towards the eEF2K mRNA was generously provided by Janssen Pharmaceuticals and cells were cultured using standard procedures in a humidified incubator at 37°C with 5% CO_2 in DMEM supplemented with 10% (v/v) FBS (fetal bovine serum), 1.5 mM glutamine, 100 units/mL penicillin and 0.1 mg/mL streptomycin. To induce knockdown of eEF2K, cells were cultured for 5 days with 1 mM isopropyl β-D-1-thiogalactopyranoside (IPTG) prior to experimentation in order to induce the knockdown of eEF2K.

Primary cultures of cortical neurons were isolated as previously described (50). Cortices were isolated in ice cold Hanks' balanced salt solution from P0 or P1 eEF2K-KO or WT mice. Tissue was gently minced and digested in Neurobasal medium (NM) containing papain (20 U/mL) and 0.32 mg/mL of L-cysteine at 37°C for 20 min followed

Molecular and Cellular Biology

by 31°C for an additional 20 min. Tissue was then washed once in NM containing 1 mg/mL each of BSA and soybean trypsin inhibitor (STI) then incubated at 37°C for 2 min in NM containing 10 mg/mL each of BSA and STI. The dissociated tissue was then washed once in NM and triturated with fire-polished glass pipettes. Cells were then washed in NM and passed through a 40 μm cell strainer after which they were counted and plated onto poly-D-lysine coated culture dishes at 1500-2000 cells/mm^2. After 1 h, the overlying medium was removed and replaced with NM containing 2% B27 supplement, 0.5 mM L-glutamine and 100 U/mL penicillin/streptomycin. One-half of the medium was replaced with fresh medium every 3-4 days. Cells were used in experiments at day-*in-vitro* 7.

Hypoxic culture conditions (1% or 0.1% (v/v) O_2) were achieved in a custom-designed hypoxic flush chamber (Billups and Rothenberg, Inc.) by infusion of a preanalyzed gas mixture (1% oxygen, 5% CO_2, 94% N_2 or 1000ppm oxygen/5% CO_2/nitrogen 200 bar) (BOC Ltd.). All experiments were performed with exponentially growing cells that had been plated at approximately 60% cell density and then made hypoxic 18 to 24 h later.

Cell lysis and analyses of samples

For Western blot analyses, cells were extracted into buffer consisting of 50 mM β-glycerophosphate, pH 7.5; 1 mM EGTA; 1 mM EDTA; 1% (v/v) Triton X-100; 1 mM Na_3VO_4; 0.1% (v/v) β-mercaptoethanol; protease inhibitors (leupeptin, pepstatin and antipain, each 1 μg/mL). Lysates were centrifuged at 13,000 rpm to remove debris. Protein

Molecular and Cellular Biology

155 concentrations in the resulting supernatants were determined as described (2). In all cases,
156 the same amount of total protein was applied to each lane of a given gel.
157
158

Molecular and Cellular Biology

Analysis of binding of eEF2K to CaM–Sepharose

To study further the interaction of eEF2K with CaM, CaM–Sepharose-binding experiments were performed using wild-type GST–eEF2K, W99A, W99L and D97A. The expressed proteins were treated overnight at 4°C with PreScission protease (20 U/ml) to cleave the GST tag. Cleaved proteins were isolated by adding glutathione resin (GE Healthcare) to remove the PreScission protease and the cleaved GST tag. 1 µg of each sample, in 50 mM (pH 7.5) and 150 mM NaCl, was applied to CaM–Sepharose™ 4B (GE Healthcare) pre-equilibrated in 50 mM MOPS (pH 7.5) and 150 mM NaCl; and either 2 mM $CaCl_2$ or 4 mM EDTA and incubated for 30 min at 4°C. The resin was washed three times with the appropriate buffer. Samples were analyzed by SDS-PAGE and western blotting using anti-GST.

Protein synthesis measurements

Briefly, cells were incubated in the presence of [^{35}S]methionine/cysteine to a final (radioactive) concentration of 10 µCi/ml for 30 min. After incubation, the medium was removed completely and the cells were washed with ice-cold PBS and lysed using a standard procedure (as described in *Cell culture and treatment*). The protein concentrations in the extracts measured using the Bradford method. Samples of lysate were applied to 3MM filter papers (Whatman) and allowed to dry at room temperature. After three brief washes with 5% (w/v) trichloracetic acid, two at 100°C and one in ethanol, filters were again dried. Incorporated radioactivity was measured by scintillation counting.

Molecular and Cellular Biology

ATP measurements

To assess ATP levels the CellTiter-Glo® Luminescent Cell Viability Assay (Promega) was used according to manufacturer's instructions to quantitate the ATP present.

Assays for eEF2 Kinase

eEF2 kinase was assayed as described earlier (4) with the following modifications. HEK 293 cells overexpressing eEF2K were harvested in high Ca^{2+} buffer (50 mM HEPES pH 7.4; 50 mM NaCl; 50 mM β-glycerophosphate; 0.3% (w/v) CHAPS; and 1 mM $CaCl_2$) in order to maintain the eEF2 kinase-CaM interaction. 10 ng of cell lysate was used per reaction in a total volume of 40 µl containing 20 mM **3-**(N-morpholino)propanesulfonic acid (MOPS), pH 7.0; containing 5 mM $MgCl_2$; 2 mM EDTA; 1 mM dithiothreitol; 2% (v/v) glycerol; 4.14 mM $CaCl_2$/5 mM EGTA (free Ca^{2+} = 1 µM at pH 7) in the presence of purified eEF2 (2 µg) and [γ-^{32}P]ATP. Activity was assayed at 30°C. The reaction was stopped by the addition of SDS-PAGE sample buffer, and the incorporation of ^{32}P into eEF2 was determined by SDS-PAGE followed by staining the gel with Coomassie brilliant blue and fluororadiography using a Typhoon phosphorimager (GE Healthcare). To measure the activity of endogenous eEF2K, 1 µg of cell lysate was used per reaction. The eEF2 kinase was IP'd with antibodies raised against either eEF2 kinase or the FLAG epitope, as appropriate, and beads were washed 4x in extraction buffer containing 1 mM Ca^{2+}-ions.

To assess the activity of recombinant eEF2K, GST-tagged eEF2K or point mutants were expressed in *E. coli* (Rosetta™(DE3)pLysS) and purified as previously described (38).

Assays of eEF2K activity were performed using buffer B [50 mM MOPS, pH 7.0 (unless stated otherwise), 20 μg/ml CaM (where present), 5 mM $MgCl_2$, 14 mM 2-mercaptoethanol, 0.67 mM $CaCl_2$, 2 mM EDTA, 0.4 mM EGTA, 1 mM benzamidine, and 1 mM each of leupeptin and pepstatin]. Reactions, in a total volume of typically 20 μl, contained 1 μg of purified eEF2 and were initiated by adding [γ-^{32}P]ATP (final concentration 0.1 mM, 1 μCi per reaction). Reactions were incubated at 30°C for times up to 30 min and then SDS/PAGE sample buffer was added. Samples were immediately heated at 95°C for 5 min to denature the proteins and stop the reaction. Products were analysed by SDS/PAGE (10% gel) and, after staining with Coomassie Brilliant Blue, gels were placed into destain/fixing solution (50% (v/v) methanol and 10% (v/v) acetic acid). Gels were then placed on Whatman 3MM paper, covered with Saran wrap and dried on a vacuum gel dryer. Radioactivity was detected using a phosphorimager (Typhoon, GE Healthcare).

Assays of eEF2K activity against the MH-1 peptide were performed in buffer B essentially as described (36) using 300 μM peptide and 100 ng of recombinant eEF2K. Filters were immediately placed in approximately 300 mL (for up to 25 filters) of 75 mM orthophosphoric acid and washed thrice more in similar volumes of the same. They were then rinsed in ethanol and dried in an oven at 100°C. Radioactivity was determined using the Čerenkov method.

Molecular and Cellular Biology

Isothermal titration calorimetry

Isothermal titration calorimetry measurements were carried out using an iTC_{200} MicroCalorimeter (GE Healthcare Bio-Sciences) at 25°C. eEF2K peptides corresponding to the wild-type eEF2K sequence (residues 78-100) were synthesized and purified to >95% purity (ChinaPeptides, Shanghai). Calmodulin and all peptides were prepared and dialyzed in the same buffer (20mM piperazine-N,N′-bis(2-ethanesulfonic acid), 150 mM KCl, 10 mM $CaCl_2$, pH 7.5). Ligand was titrated into protein solution at molar ratios of 10:1 corresponding to approximately 220 µM ligand (peptide) and 19 µM protein (CaM). Each experiment consisted of a first injection of 0.3 µl followed by 39 injections of 1 µl of peptide solution into the cell, while stirring at 800 rpm. Control titrations (peptide into buffer) were measured. Data acquisition/analysis were performed using the Origin Scientific Graphing and Analysis software package (OriginLab). Data analysis was performed by generating a binding isotherm and best fit using the following parameters: N (number of sites), Δ H (cal/mol), Δ S (cal/mol/deg), and K (binding constant, M^{-1}).

Protein digestion, analysis by mass spectrometry and data processing.

Proteomic analyses were carried out by the University of Leicester Proteomics Facility (PNACL). Bands of interest were excised from the gel, and in-gel trypsin digestion was carried out upon each (45). Each slice was destained using 200 mM ammonium bicarbonate/20% acetonitrile, followed by reduction (10 mM dithiothreitol, Melford Laboratories Ltd., Suffolk, UK), alkylation (100 mM iodoacetamide, Sigma, Dorset, UK) and enzymatic digestion with trypsin (sequencing grade modified porcine trypsin, Promega, Southampton, UK) in 50 mM triethylammonium bicarbonate (Sigma) using an automated

digestion robot (Multiprobe II Plus EX, Perkin Elmer, UK). After overnight digestion, samples were acidified using formic acid (final concentration 0.1% (v/v)).

LC-MS/MS was carried out using an RSLCnano HPLC system (Dionex, UK) and an LTQ-Orbitrap-Velos mass spectrometer (Thermo Scientific). Samples were loaded at high flow rate onto a reverse-phase trap column (0.3 mm i.d. x 1 mm), containing 5 µm C18 300 Å Acclaim PepMap medium (Dionex) maintained at a temperature of 37°C. The loading buffer was 0.1% formic acid / 0.05% trifluoroacetic acid / 2% acetonitrile.

Peptides were eluted from the trap column at a flow rate of 0.3 µL/min and through a reverse-phase capillary column (75µm i.d. x 250mm) containing Symmetry C18 100 Å medium (Waters, UK) that was manufactured in-house using a high pressure packing device (Proxeon Biosystems, Denmark). The output from the column was sprayed directly into the nanospray ion source of the LTQ-Orbitrap-Velos mass spectrometer.

The LTQ-Orbitrap-Velos mass spectrometer was set to acquire a 1 microscan FTMS scan event at 60000 resolution over the m/z range 350-1250 Da in positive ion mode. Accurate calibration of the FTMS scan was achieved using a background ion-lock mass for polydimethylcyclosiloxane (445.120025 Da). Subsequently up to 10 data dependent HCD MS/MS were triggered from the FTMS scan. The isolation width was 2.0 Da, normalized collision energy 40.0, and activation time 10 ms. Dynamic exclusion was enabled.

Molecular and Cellular Biology

Mutagenesis of eEF2K

The cDNA encoding human eEF2K was cloned into a pcDNA3.1 vector for expression of FLAG-tagged eEF2K in HEK-293 cells. Mutagenesis of proline 96 or proline 98 in human eEF2 kinase to alanine was performed by PCR using "QuikChange®" (Stratagene). The forward primer for P96A was 5′- GAAGGCCAAGCACATGGCCGACCCCTGGGCTG -3′, and the reverse primer for P96A was 5′-CAGCCCAGGGGTCGGCCATGTGCTTGGCCTTC-3′. The forward primer for P98A was 5′-GCACATGCCCGACGCCTGGGCTGAGTTC -3′, and the reverse primer for P98A was 5′-GAACTCAGCCCAGGCGTCGGGCATGTGC-3′.

Reproducibility and statistical analysis of data.

All experiments were conducted at least three times, with similar data being obtained in each case. For immunoblots, a typical set of data is shown in each case. Quantitation of immunoblot data was achieved using the LiCor Odyssey software**.**

Numerical data are expressed as the mean ±S.E.M. for the indicated number of individual experiments. Wherever appropriate, the statistical significance of the data was assessed using a student's t-test, a one-way ANOVA followed by Dunnets post test or a two-way ANOVA followed by a Bonferroni post-hoc test, as described in the figure legends, using Graph Pad prism 6 software. * <0.05, ** <0.01, *** <0.001, **** <0.0001.

Results

Hypoxia elicits a delayed increased in eEF2 phosphorylation

Subjecting HCT116 colorectal carcinoma cells to hypoxia caused a small but consistent increase in eEF2 phosphorylation at 2h and a gradual, but more pronounced increase by 8-16 h (Fig. 1A). Our findings are distinct from an earlier study which reported a rapid increase in eEF2K phosphorylation during hypoxia (42); our data also reveal the existence of a second, slower and much more marked rise in eEF2 phosphorylation. The rapid changes in eEF2 phosphorylation that they observed likely reflect different regulatory inputs into eEF2.

Hypoxia also caused an increase in eEF2 phosphorylation in mouse embryonic fibroblasts (MEFs), HeLa cells or primary cortical neurons by similar times (Fig. 1B-D). This was not observed in cells from mice in which the *EEF2K* gene has been disrupted (Fig. 1B; see also Fig. 2A,B), indicating that hypoxia-induced eEF2 phosphorylation requires eEF2K (and is not catalysed by AMPK, which has been reported to phosphorylate eEF2 (21)).

Although hypoxia (10,46) or inhibition of PHDs using dimethyloxalylglycine (DMOG) has previously been shown to increase eEF2 phosphorylation, through PHD2 (42), the underlying mechanisms remain unknown. The delayed nature of this effect was of particular interest as hypoxia might increase the expression of eEF2K, e.g., at a transcriptional level via HIF1α, which mediates the induction of a gene expression program that helps cells adapt to hypoxia (34) or by stabilising the eEF2K protein itself (analogous

Molecular and Cellular Biology

to the stabilisation of HIF1α). However, there was no significant increase in eEF2K protein levels in cells subjected to hypoxia (Fig. 1A-C); if anything, in some cases, eEF2K levels actually fell (Fig. 1A), as seen under other conditions where eEF2K is activated (27,49). Thus, the hypoxia-induced phosphorylation of eEF2 does not appear to result from stabilisation of eEF2K or induction of its expression. The simplest alternative explanation is that the intrinsic activity of eEF2K increases during hypoxia and this is examined below.

Hypoxia-induced phosphorylation of eEF2 does not require signaling via AMPK or mTORC1

We first explored whether known upstream regulators of eEF2K were involved in the hypoxia-induced increase in eEF2 phosphorylation. Members of the p38 MAP kinase family are often activated during cell stresses and can phosphorylate eEF2K, although they provide a negative input to eEF2K activity rather than stimulating it (25,26). Nevertheless, we examined whether p38 MAPK was activated (phosphorylated) during hypoxia in HCT116 cells, MEFs and HeLa cells. A transient increase was seen in HCT116 cells, well before the rise in eEF2 phosphorylation, and no change was seen in the other cells tested (Fig. 1A-C).

Hypoxia and the consequent ATP depletion can stimulate AMPK which can, in turn, activate eEF2K (3,22). For example, hypoxia caused a delayed activation of AMPK in HCT116 cells, as judged from the phosphorylation of a well-established AMPK substrate, acetyl-CoA carboxylase (ACC; Fig. 1A), although this appeared to lag behind the increase in phospho-eEF2 suggesting it may not be a causative event in regulating eEF2 here. An

Molecular and Cellular Biology

inhibitor of AMPK, MRT199665 (9), did not prevent the hypoxia-induced phosphorylation of eEF2 (Fig. 3A). Furthermore, hypoxia still increased eEF2 phosphorylation in AMPKα double-knockout cells (Fig. 3B). Thus, the hypoxia-induced phosphorylation of eEF2 is independent of AMPK, ruling out that it is directly mediated by AMPK or via, e.g., AMPK-induced inactivation of mTORC1 signaling (18,23). We noted that the levels of eEF2K protein and *EEF2K* mRNA are both lower in AMPK-DKO cells (Fig. 3B,C), suggesting that AMPK that may positively regulate eEF2K expression.

Inhibition of proline hydroxylases induces the phosphorylation of eEF2 independently of altered mTORC1 or AMPK signaling

To explore how PHDs regulate eEF2 and eEF2K, we made use of the PHD inhibitor DMOG. Treatment of HCT116 or HeLa cells with DMOG increased the phosphorylation of eEF2, often markedly (Fig. 1E,F; and 3D,E,G). However, eEF2K levels did not increase, similar to the situation in hypoxia (Fig. 1A-C). Since DMOG affects both prolyl hydroxylases and related enzymes such as asparaginyl hydroxylase, we also tested the effects of a specific PHD inhibitor, FG-4497 (41). FG-4497 also enhanced eEF2 phosphorylation in HeLa cells (Fig. 1G). Since use of FG-4497 requires that cells are maintained in lower serum (2%) than usual (10%), which itself tends to raise p-eEF2 levels, the increase caused by FG-4497 is less than seen with DMOG (which can be used on cells in higher serum concentrations). However, the final level of p-eEF2 is similar with either reagent, confirming that DMOG affects eEF2 phosphorylation by inhibiting PHDs.

DMOG was also unable to increase eEF2 phosphorylation in A549 cells where eEF2K had been knocked down using shRNA (Fig. 3D) or in eEF2K$^{-/-}$ MEFs (Fig. 3E), showing that here the phosphorylation of eEF2 is also mediated by eEF2K. The effect of DMOG was relatively slow, typically requiring 4-6 h. In contrast, AZD8055 (8), which blocks the mTOR pathway that negatively regulates eEF2K activity (39), induced a faster increase in eEF2 phosphorylation (Fig. 3G). This is consistent with the effect of DMOG not being due to impaired mTORC1 signaling, a point which is explored in detail below, although alternative explanations are possible. It should also be noted that, while hypoxia did decrease mTORC1 signaling in HCT116 cells (as judged from the decrease in phosphorylation of ribosomal protein S6 at Ser240/244, well-known substrates for the p70 S6 kinases which are activated by mTORC1; Fig. 1A), this effect was much more rapid than the rise in phospho-eEF2, which is inconsistent with a direct link between them.

The robust induction of eEF2 phosphorylation by DMOG in HCT116 cells was not blocked by MRT199665 (9) again indicating that AMPK is not involved (Fig. 3F). However, DMOG did increase the phosphorylation of acetyl-CoA carboxylase, an AMPK substrate, and MRT199665 blocked this (Fig. 3F), implying that DMOG increases AMPK activity; although the mechanism underlying this is unclear. AMPK is activated by phosphorylation (at Thr172) by the protein kinase LKB1, which is not present in HeLa cells (47). DMOG failed to activate AMPK in this cell-type, as judged by the phosphorylation status of its substrate ACC (Fig. 1F), indicating that the effect of DMOG on AMPK probably requires LKB1.

Hypoxia or DMOG can each impair mTORC1 signaling via the HIF1α-mediated induction of REDD1, a positive regulator of the TSC1/TSC2 complex that inhibits mTORC1 signaling (5,15). Since mTORC1 signaling negatively regulates eEF2K, hypoxia or DMOG might induce eEF2 phosphorylation by relieving this inhibitory input from mTORC1. In HCT116 colorectal carcinoma cells, MEFs and HeLa cells, hypoxia or DMOG treatment did indeed inhibit mTORC1 signaling, as judged by the decreased phosphorylation of ribosomal protein S6 (RpS6; Fig. 1A,C,F), a substrate for the S6 kinases which are activated by mTORC1, and of 4E-BP1, another mTORC1 substrate (Fig. 1C). Since the effects of hypoxia on mTORC1 signaling are mediated via the TSC1/2 complex (5), we used TSC2-null cells to eliminate this input. Hypoxia or DMOG did not affect S6 phosphorylation in $TSC2^{-/-}$ MEFs, but still induced the phosphorylation of eEF2 (Fig. 4A,B), albeit more slowly, without the initial rise, likely reflecting the high activity of mTORC1 signaling (and lower eEF2k activity) in these cells. This implies the slow phase of the effect of DMOG is not mediated via impaired mTORC1 signaling. PHDs also play a role in the activation of mTORC1 signaling by amino acids (15). However, DMOG did not affect mTORC1 signaling (S6 phosphorylation) in $TSC2^{-/-}$ cells where this input is still intact, therefore the increased phosphorylation of eEF2 does not reflect this role of PHDs in cellular regulation. Taken together, these data demonstrate that hypoxia and DMOG treatment enhance eEF2 phosphorylation independently of inhibition of mTORC1 signaling.

eEF2K mRNA levels can be reciprocally regulated by mTORC1 and hypoxia

We noted that eEF2K protein levels are lower in TSC2$^{-/-}$ MEFs than in wild-type cells and that, in these cells, they did increase following DMOG treatment (Fig. 4A). To study this further, we measured the levels of the *EEF2K* mRNA. *EEF2K* mRNA levels were markedly lower in TSC2$^{-/-}$ cells than wild-type MEFs (Fig. 4C), and increased in response to DMOG treatment in TSC2$^{-/-}$ but not in WT MEFs (Fig. 4C). These effects, seen only in TSC2$^{-/-}$ cells where mTORC1 signaling is very active, suggest that DMOG may counter an inhibitory effect of hyperactivated mTORC1 signaling on eEF2K expression. DMOG induced another HIF1α-regulated mRNA, *GLUT1*, to a similar degree in both cell lines, i.e., irrespective of their TSC2 status (Fig. 4D). Acroflavine, which inhibits HIF1α dimerization (29), blocked the DMOG-induced rise in eEF2K levels (Fig. 4E), suggesting this increase is mediated via HIF1α. However, analysis of the promoter region of the mouse *EEF2K* gene failed to reveal any consensus binding sites for HIF1α.

Thus, the expression of the mRNA for *EEF2K* is probably regulated in multiple ways, e.g., downstream of AMPK, and in some settings by mTORC1 signaling and HIF1α; further work, beyond the scope of this study, is required to define the mechanisms involved here.

Hypoxia or DMOG-treatment enhances the intrinsic activity of eEF2K

Our data show that, in cells other than the single example of TSC2-null MEFS, hypoxia or DMOG treatment enhance eEF2 phosphorylation without increasing the levels of eEF2K protein. This suggested that the intrinsic activity of eEF2K may be enhanced under this condition. To test this, we assayed eEF2K activity in lysates of HeLa or HCT166 cells, with or without an episode of hypoxia. As shown in Fig. 5A, hypoxia did indeed increase eEF2K activity. Similarly, higher eEF2K activity was observed following treatment of HEK293 cells or MEFs with DMOG although total levels of eEF2K were unchanged (Fig. 5B-D). To confirm conclusively that this change did reflect the activation of eEF2K, not, e.g., stimulation of a (hypothetical) alternative kinase or a change in phosphatase activity against eEF2, eEF2K was immunoprecipitated (IP'd) from MEF lysates prior to the assay, under mild conditions, and in the presence of Ca^{2+}-ions, where CaM remains associated with eEF2K (4). Again, higher activity was observed in samples from DMOG-treated cells than in untreated controls (Fig. 5D; right hand part), confirming that treating cells with DMOG does increase the activity of eEF2K. It should be noted that the data for DMOG and for $TSC2^{-/-}$ MEFs (e.g., Fig. 4A,B) rule out inputs to the increase in eEF2K activity from other effects of hypoxia or impaired mTORC1 signaling, respectively.

Finally, it was possible, as is the case in response to elevated cAMP levels (40), that eEF2K activity became independent of Ca^{2+}-ions in DMOG-treated cells. However, eEF2K activity still showed a strong requirement for Ca^{2+}-ions in samples from DMOG-treated cells (Fig. 5B).

Molecular and Cellular Biology

eEF2K is subject to hydroxylation on a highly conserved proline

Given that neither mTORC1 nor AMPK was involved in the effects reported here, and that eEF2K levels were not increased by DMOG or hypoxia, we examined whether eEF2K is itself subject to hydroxylation. To do this, eEF2K was immunoprecipitated from normoxic cells and then subjected to tryptic digestion followed by mass spectrometric analysis. This revealed the presence of one peptide, i.e., HMPDPWAEFHLEDIATER, that showed a mass shift of 32 Da, which is equivalent to two additional oxygen atoms (mass of observed peptide, 2224.8, compared to the mass predicted from the sequence, 2192.35). Inspection of the mass spectrum shows that one of these oxygen atoms corresponds to the oxidation of the only methionine in this peptide (cf. Table 1) which can occur during sample preparation. The hydroxylated peptide was observed in five separate experiments with material from normoxic cells, whereas the non-hydroxylated version of the peptide was not observed under this condition. The peptide identified corresponds to a region between the CaM-binding motif (12,37) and the catalytic domain of eEF2K. It contains two proline residues, Pro96 and Pro98 (Fig. 6A).

It was important to pinpoint which proline in this peptide is modified. Fig. 6B shows a theoretical spectrum based on this peptide where either Pro96 (yielding peptide y16+2H) or Pro98 (y14+2H) is considered to be hydroxylated. The data in Fig. 6C and Table 1 show the y-ion series appearing at y14 m/z = 865.4 (2+) and the b-ion series at b5 *m/z* = 305.6 (2+). This assigns the hydroxylation event unambiguously to proline 98 and rules out hydroxylation of Pro96 or any other similar modification, such as double oxidation of methionine to the sulfone (Table 1).

Molecular and Cellular Biology

Samples of eEF2K derived from cells subjected to hypoxia for 24 h (to allow replacement of hydroxylated eEF2K by the non-hydroxylated protein) showed only a lighter version of this peptide, which unlike that from normoxic cells, was not hydroxylated on either proline residue. These data show that this peptide, and Pro98 in particular, is not hydroxylated under hypoxic conditions.

Pro98 and the two adjacent residues are highly conserved among vertebrate eEF2K sequences and, strikingly, given the low overall sequence identity in this region of eEF2K, are even conserved in eEF2K from nematode worms (Table 2). Given that Pro98 is close to the CaM binding site, we asked whether treating cells with DMOG, to prevent hydroxylation, affected the ability of CaM to activate eEF2K.

Cells were transfected with a vector encoding FLAG-tagged eEF2K. To ensure that, where appropriate, that none of the eEF2K under study was hydroxylated, cells were treated with DMOG for the entire period during which the ectopic eEF2K was expressed. Lysates were prepared using buffer containing Ca^{2+}-ions (where some CaM remains associated with eEF2K). Under these conditions eEF2K from DMOG-treated cells showed higher activity than from control cells (Fig. 7A, top part); since expression of FLAG-eEF2K is much higher than the endogenous protein (Fig. 7B, right hand part), the assay reflects the activity of the FLAG-eEF2K.

This difference between control and DMOG-treated samples could reflect decreased association of eEF2K with CaM or lower ability of CaM to activate eEF2K. To evaluate this, excess CaM was added to lysates from control or DMOG-treated cells; this strongly stimulated eEF2K activity towards eEF2 (Fig. 7A, middle part). Importantly, even in the

Molecular and Cellular Biology

presence of excess CaM, the activity of eEF2K from DMOG-treated cells was substantially higher than that of eEF2K from control cells (Fig. 7A), where Pro98 is hydroxylated. This indicates that CaM is less able to stimulate eEF2K from control cells where Pro98 is hydroxylated.

Similarly, in lysates from MEFs, addition of a large amount of CaM to the assay did not eliminate the difference in activity of eEF2K from control vs. DMOG-treated cells (Fig. 5D). The clear implication of these data is that hydroxylation of eEF2K likely impairs the extent to which CaM stimulate eEF2K, thus limiting its activity.

To test specifically the role of hydroxylation of Pro98 in controlling eEF2K activity, Pro98 was mutated to alanine, which cannot be hydroxylated and is otherwise probably the most similar residue to proline. We also created eEF2K[Pro96Ala] as a (negative) control. The WT and mutant eEF2K proteins expressed at similar levels in HEK293 cells and their expression was not affected by DMOG treatment, confirming that PHD inhibition does not alter the stability of eEF2K (Fig. 7B). Since FLAG-eEF2K protein levels were much higher than those of endogenous eEF2K (Fig. 7B, right hand part), we could reliably assess FLAG-eEF2K activity in cell lysates (where sufficient CaM is already present). DMOG pre-treatment of the cells caused similar increases in the activity of WT and eEF2K[P96A] (Fig. 7C,D). In contrast, the activity of eEF2K[P98A] was already higher than that of wild-type eEF2K in samples from normoxic cells and, more importantly, DMOG did not increase it further (Fig. 7C,D). The activities of WT eEF2K and eEF2K[P98A] were strictly dependent upon Ca/CaM in control and DMOG-treated conditions (Fig. 7E). These data

Molecular and Cellular Biology

suggest that hydroxylation of Pro98 under normoxic conditions limits eEF2K activity, while the absence of hydroxylation permits a higher level of activity.

Hydroxylation of Pro98 impairs binding of eEF2K to CaM and its activation by CaM

The proximity of Pro98 to the CaM-binding site suggested its hydroxylation might affect eEF2K's interaction with CaM. We therefore used isothermal titration calorimetry (ITC) to study the binding of CaM to synthetic peptides including the CaM-binding site of eEF2K; we used peptides corresponding to residues 78-100 of human eEF2K and containing, at the position equivalent to residue 98, either proline or hydroxyproline. The unmodified peptide bound to CaM with an affinity of 66±9 nM, while binding to 78-100(HO-Pro98) was somewhat weaker (K_d, 123±3 nM; Fig. 8A,B; Table 3), showing that the hydroxylation of Pro98 does interfere with CaM binding, but only modestly. To assess whether hydroxylation affected the overall ability of eEF2K to bind CaM, HEK293 cells were transfected with a vector for FLAG-eEF2K. eEF2K was IP'd from control or DMOG-treated cells (Fig. 8C). No difference was observed in the amount of CaM which co-purified with the FLAG-tagged eEF2K, consistent with modest change in the affinity for CaM shown by the ITC data.

If the altered affinity of eEF2K for CaM sufficed to explain its control by proline hydroxylation/DMOG, then adding additional, saturating levels of CaM should overcome the difference in the affinity for CaM of eEF2K from control compared to hypoxic or DMOG-treated cells. However, the data reported in Figs. 6D, 8C show that adding excess

CaM did not bring the activity of eEF2K from control cells up to the higher level seen for DMOG-treated cells, indicate that binding of CaM to eEF2K does not limit its activity here. Thus, the hydroxylation of Pro98 probably restricts the activity of eEF2K by decreasing its capacity to be fully activated by CaM and/or its maximal activity.

As noted above, Pro98 lies in the 'linker' region between the CaM-binding- and catalytic domains of eEF2K, which is strongly conserved across vertebrate eEF2K sequences suggesting it might play an important role (Fig. 6A). Indeed, Pro98 and its flanking residues (Asp97 and Trp99 in human eEF2K) are even conserved in eEF2K from distantly-related nematodes. To test the roles of these residues, we mutated them to alanines, and also, more conservatively, mutated W99 to leucine, another hydrophobic residue. eEF2K[W97A], [W99A] and [W99L] all still bound to CaM (Fig. 8D), likely because they lie beyond the identified CaM binding site. In contrast, in the presence of CaM, these mutants each showed substantially lower activity than WT eEF2K against MH-1, an established peptide substrate for eEF2K (37) (Fig. 8E). Indeed, eEF2K[W99A] almost entirely failed to undergo activation by Ca^{2+}/CaM when its activity was assessed against this peptide or eEF2 (Fig. 8E,F). Thus, these highly conserved residues in the 'linker' region between the CaM-binding site and the catalytic domain apparently play a key role in coupling CaM binding to the stimulation of eEF2K activity, consistent with a role of hydroxylation of Pro98 in influencing the activation of eEF2K by CaM.

Taken together, our data indicate that hydroxylation of Pro98 both somewhat weakens the binding of eEF2K to CaM and impairs the ability of CaM to fully activate eEF2K (or its maximal activity). Thus, even when eEF2K is assayed in the presence of

Molecular and Cellular Biology

excess CaM, hydroxylation of Pro98 still limits its maximal activity, thereby restraining eEF2K activity during normoxia.

Since there is no known mechanism to reverse proline hydroxylation (24), the enhancement of eEF2K activity during hypoxia requires the replacement of the pre-existing hydroxylated eEF2K by newly-made, more active non-hydroxylated eEF2K protein. Importantly, the rate of accumulation of new (in this case FLAG-tagged) eEF2K is comparable to that of the hypoxia- or DMOG-induced increase in eEF2 phosphorylation (Fig. 9; cf. Fig. 1). Previous data indicate that eEF2K has a relatively short half-life (1). The nature of this control mechanism presumably explains why the effects of hypoxia or DMOG on eEF2 phosphorylation are relatively slow.

eEF2K aids the survival of neuronal cells during hypoxia

The activation of eEF2K that occurs during hypoxia is expected to restrain the rate of elongation and thereby help cells cope with the available energy supply. We therefore tested whether eEF2K plays a role in helping cells to withstand hypoxia. This condition has a particularly pronounced impact on cells or tissues which depend heavily upon oxidative metabolism (e.g., cardiomyocytes, neurons). Cardiac muscle and brain undergo oxygen deprivation during ischemia or stroke. eEF2K has previously been shown to protect cardiomyocytes against hypoxic damage (46). We therefore tested its importance in another oxygen-dependent cell-type, primary neuronal cultures from wild-type or eEF2K$^{-/-}$ mice. Following hypoxia, eEF2K$^{-/-}$ neurons showed greater depletion of ATP and increased cleavage of poly ADP-ribose polymerase (PARP) (16) compared to wild-type cells (Fig.

Molecular and Cellular Biology

10A,B). This indicates that eEF2K is cytoprotective in primary neurons as reported previously for cancer cell lines (10) (Fig. 10B). These data are consistent with the finding that, in neuronal cells subjected to hypoxia, inhibiting protein synthesis using carbimazole (which induces eEF2 phosphorylation), or other agents, preserved ATP content and prevented cell damage (30). These data underline the importance of eEF2K for resistance to oxygen deprivation. Interestingly, recent work has revealed that eEF2K is cytoprotective during nutrient starvation (31). This key role for eEF2K in helping cells withstand nutrient deficiency likely reflects the facts that protein synthesis consumes a large proportion of the energy generated by oxidative metabolism (6) and that eEF2 phosphorylation inhibits translation elongation, reducing the energy demands.

It was important to assess whether the observed phosphorylation of eEF2 was associated with inhibition of protein synthesis. It is not possible to do this for hypoxia, since opening the hypoxic chamber to add the radiolabel admits oxygen, abrogating the hypoxia. It was therefore more appropriate to study the effect of DMOG; however, this generally impairs mTORC1 signaling, which in turn controls other components of the translational machinery, making it impossible to interpret data from wild-type (or even eEF2K$^{-/-}$) MEFs. To avoid this complication, we used TSC2$^{-/-}$ MEFs, where DMOG affects neither mTORC1 signaling (as assessed by the phosphorylation of S6) nor the phosphorylation of eIF2, another key regulator of protein synthesis (Fig. 10C). DMOG substantially inhibited protein synthesis in TSC2$^{-/-}$ MEFs (Fig. 10D), consistent with the concept that the phosphorylation of eEF2 serves to restrict ATP consumption, thereby favouring cell survival. It is important to note that the complete inhibition of protein

Molecular and Cellular Biology

593 synthesis during hypoxia is inappropriate given that it is crucial that for some proteins to
594 continue to be made to allow cells to adapt to this condition (e.g., HIF1α; see (48)).

595

Molecular and Cellular Biology

Discussion

Here we describe the first example of oxygen-dependent proline hydroxylation regulating a protein (eEF2K) that is directly involved in regulating a major energy-consuming process (protein synthesis). Hydroxylation of eEF2K during normoxia restrains its activity, such that its activity is enhanced during hypoxia, a response that will serve to decrease the demand for ATP and GTP for translation elongation. Importantly, Pro98 is not hydroxylated in eEF2K from hypoxic or DMOG-treated cells. eEF2K is also the first protein kinase whose activity is known to be regulated by proline hydroxylation; although IκB kinase-β is also subject to this modification, it appears primarily to regulate the levels of this kinase rather than its intrinsic activity (11). Two very recent studies showed that ribosomal protein S23 is subject to proline hydroxylation (33,44), but, unlike the effects reported here, this modification is appears not to be involved in the overall control of translation during hypoxia.

The fact that the modified residue in eEF2K, Pro98, and neighbouring residues are completely conserved through evolution from nematodes to primates suggests this is an ancient mechanism for regulating protein synthesis in response to oxygen deficiency. Our findings also point to a key role for residues in the linker region between the CaM-binding site in eEF2K and its catalytic domain in its activation by CaM. Given the high demand of protein synthesis for cellular energy (6), it makes clear physiological sense that hypoxia should induce the phosphorylation and inhibition of eEF2 to reduce the energy needs of protein synthesis. Ideally, it would be useful to show that WT eEF2K inhibits protein synthesis to a lesser extent than the Pro98Ala mutant during normoxic conditions within

Molecular and Cellular Biology

cells; however, more active mutants of eEF2K inhibit their own synthesis (or that of a co-transfected reporter) which are therefore expressed at markedly lower levels than for less active variants (13,36). This unfortunately makes it very hard to interpret the data from such experiments.

Our findings also reveal that the level of expression of the *EEF2K* mRNA is lower in cells lacking active AMPK or with hyperactivated mTORC1 signaling, pointing to transcriptional control of eEF2K expression by nutrient-sensitive signaling pathways. Interestingly, nutrient deprivation increases the expression of the *EEF2K* mRNA in mammalian cells and in *C. elegans* (31), consistent with enhanced expression of this cytoprotective kinase as a widespread response to lack of nutrients. In contrast, oxygen deprivation or inhibition of PHDs did not increase the levels of eEF2K, except in the single example of $TSC2^{-/-}$ cells, where constitutive mTORC1 signaling normally appears to repress eEF2K expression. Oxygen availability thus generally appears to promote the activation, rather than the expression level, of eEF2K.

The replacement of pre-existing, hydroxylated and less active eEF2K by more active, non-hydroxylated eEF2K presumably allows cells to adapt to low oxygen conditions, such that enhancement of eEF2K activity no longer has to rely on inputs from inhibition of mTORC1 or activation of AMPK. This resets the activity of eEF2K, and thus eEF2 phosphorylation, at a higher level, providing a mechanism to allow cells to adapt to reduced oxygen availability by stably enhancing the activity of a protein kinase that slows down translation elongation. The activation of AMPK or inhibition of mTORC1 signaling, which can each acutely activate eEF2K, likely serves to provide short-term modulation of

Molecular and Cellular Biology

eEF2K activity. The long-term adaptive response revealed in this study is distinct from the rapid responses to PHD inhibition reported recently (42).

These data, together with earlier findings showing cytoprotective roles for eEF2K in hypoxic cardiac muscle cells (10) and in response to starvation for amino acids and glucose (see, e.g., (31)), indicate that eEF2K helps to defend cells against the adverse effects of deficiencies in diverse nutrients. eEF2K may therefore be a useful target in tackling poorly-vascularised solid tumors, regions of which may become hypoxic, and require eEF2K to allow cell survival (32).

Molecular and Cellular Biology

ACKNOWLEDGEMENTS

We are grateful to Professor Philip Cohen (Dundee) for kindly providing MRT199665, Dr Andrew Bottrill (Leicester) for MS analyses and DR Paul Skipp (Southampton) for advice. $TSC2^{-/-}$ and AMPK-null cells were generous gifts from Drs David Kwiatkowski (Boston) and Benoit Viollet (Paris), respectively. This work was supported by funding to CGP from the Wellcome Trust (Grant number 086688). The authors have no conflicts of interest to disclose.

Reference List

1. **Arora, S., J. M. Yang, and W. N. Hait**. 2005. Identification of the ubiquitin-proteasome pathway in the regulation of the stability of eukaryotic elongation factor-2 kinase. Cancer Res. **65**:3806-3810.

2. **Bradford, M. M.** 1976. A rapid and sensitive method for the quantitation of microgram quantities of protein utilizing the principle of protein-dye binding. Anal. Biochem. **77**:248-254.

3. **Browne, G. J., S. G. Finn, and C. G. Proud**. 2004. Stimulation of the AMP-activated protein kinase leads to activation of eukaryotic elongation factor 2 kinase and to its phosphorylation at a novel site, serine 398. J. Biol. Chem. **279**:12220-12231.

4. **Browne, G. J. and C. G. Proud**. 2004. A novel mTOR-regulated phosphorylation site in elongation factor 2 kinase modulates the activity of the kinase and its binding to calmodulin. Mol Cell Biol **24**:2986-2997.

5. **Brugarolas, J., K. Lei, R. L. Hurley, B. D. Manning, J. H. Reiling, E. Hafen, L. A. Witters, L. W. Ellisen, and W. G. Kaelin, Jr.** 2004. Regulation of mTOR function in response to hypoxia by REDD1 and the TSC1/TSC2 tumor suppressor complex. Genes Dev. **18**:2893-2904.

6. **Buttgereit, F. and M. D. Brand**. 1995. A hierarchy of ATP-consuming processes in mammalian cells. Biochem. J. **312**:163-167.

7. **Carlberg, U., A. Nilsson, and O. Nygard**. 1990. Functional properties of phosphorylated elongation factor 2. Eur. J. Biochem. **191**:639-645.

8. **Chresta, C. M., B. R. Davies, I. Hickson, T. Harding, S. Cosulich, S. E. Critchlow, J. P. Vincent, R. Ellston, D. Jones, P. Sini, D. James, Z. Howard, P. Dudley, G. Hughes, L. Smith, S. Maguire, M. Hummersone, K. Malagu, K. Menear, R. Jenkins, M. Jacobsen, G. C. Smith, S. Guichard, and M. Pass**. 2010. AZD8055 is a potent, selective, and orally bioavailable ATP-competitive mammalian target of rapamycin kinase inhibitor with in vitro and in vivo antitumor activity. Cancer Res. **70**:288-298.

9. **Clark, K., K. F. MacKenzie, K. Petkevicius, Y. Kristariyanto, J. Zhang, H. G. Choi, M. Peggie, L. Plater, P. G. Pedrioli, E. McIver, N. S. Gray, J. S. Arthur, and P. Cohen**. 2012. Phosphorylation of CRTC3 by the salt-inducible kinases controls the interconversion of classically activated and regulatory macrophages. Proc. Natl. Acad. Sci. U. S. A **109**:16986-16991.

10. **Connolly, E., S. Braunstein, S. Formenti, and R. J. Schneider**. 2006. Hypoxia inhibits protein synthesis through a 4E-BP1 and elongation factor 2 kinase pathway controlled by mTOR and uncoupled in breast cancer cells. Mol. Cell Biol. **26**:3955-3965.

11. **Cummins, E. P., E. Berra, K. M. Comerford, A. Ginouves, K. T. Fitzgerald, F. Seeballuck, C. Godson, J. E. Nielsen, P. Moynagh, J. Pouyssegur, and C. T. Taylor**. 2006. Prolyl hydroxylase-1 negatively regulates IkappaB kinase-beta, giving insight into hypoxia-induced NFkappaB activity. Proc. Natl. Acad. Sci. U. S. A **103**:18154-18159.

12. **Diggle, T. A., C. K. Seehra, S. Hase, and N. T. Redpath**. 1999. Analysis of the domain structure of elongation factor-2 kinase by mutagenesis. FEBS Lett. **457**:189-192.

13. **Diggle, T. A., T. Subkhankulova, K. S. Lilley, N. Shikotra, A. E. Willis, and N. T. Redpath**. 2001. Phosphorylation of elongation factor-2 kinase on serine 499 by cAMP-dependent protein kinase induces Ca^{2+}/calmodulin-independent activity. Biochem. J. **353**:621-626.

14. **Drennan, D. and A. G. Ryazanov**. 2004. Alpha-kinases: analysis of the family and comparison with conventional protein kinases. Prog. Biophys. Mol Biol **85**:1-32.

15. **Duran, R. V., E. D. Mackenzie, H. Boulahbel, C. Frezza, L. Heiserich, S. Tardito, O. Bussolati, S. Rocha, M. N. Hall, and E. Gottlieb**. 2012. HIF-independent role of prolyl hydroxylases in the cellular response to amino acids. Oncogene.

16. **Gobeil, S., C. C. Boucher, D. Nadeau, and G. G. Poirier**. 2001. Characterization of the necrotic cleavage of poly(ADP-ribose) polymerase (PARP-1): implication of lysosomal proteases. Cell Death. Differ. **8**:588-594.

17. **Gorres, K. L. and R. T. Raines**. 2010. Prolyl 4-hydroxylase. Crit Rev. Biochem. Mol. Biol. **45**:106-124.

18. **Gwinn, D. M., D. B. Shackelford, D. F. Egan, M. M. Mihaylova, A. Mery, D. S. Vasquez, B. E. Turk, and R. J. Shaw**. 2008. AMPK phosphorylation of raptor mediates a metabolic checkpoint. Mol. Cell **30**:214-226.

19. **Hall-Jackson, C. A., D. A. Cross, N. Morrice, and C. Smythe**. 1999. ATR is a caffeine-sensitive, DNA-activated protein kinase with a substrate specificity distinct from DNA-PK. Oncogene **18**:6707-6713.

20. **Hardie, D. G., F. A. Ross, and S. A. Hawley**. 2012. AMPK: a nutrient and energy sensor that maintains energy homeostasis. Nat. Rev. Mol. Cell Biol. **13**:251-262.

21. **Hong-Brown, L. Q., C. R. Brown, D. S. Huber, and C. H. Lang**. 2008. Lopinavir impairs protein synthesis and induces eEF2 phosphorylation via the activation of AMP-activated protein kinase. J. Cell Biochem. **105**:814-823.

22. **Horman, S., G. J. Browne, U. Krause, J. V. Patel, D. Vertommen, L. Bertrand, A. Lavoinne, L. Hue, C. G. Proud, and M. H. Rider**. 2002. Activation of AMP-activated protein kinase leads to the phosphorylation of elongation factor 2 and an inhibition of protein synthesis. Curr. Biol. **12**:1419-1423.

23. **Inoki, K., T. Zhu, and K. L. Guan**. 2003. TSC2 mediates cellular energy response to control cell growth and survival. Cell **115**:577-590.

24. **Kaelin, W. G., Jr. and P. J. Ratcliffe**. 2008. Oxygen sensing by metazoans: the central role of the HIF hydroxylase pathway. Mol. Cell **30**:393-402.

25. **Knebel, A., C. E. Haydon, N. Morrice, and P. Cohen**. 2002. Stress-induced regulation of eEF2 kinase by SB203580-sensitive and -insensitive pathways. Biochem. J. **367**:525-532.

26. **Knebel, A., N. Morrice, and P. Cohen**. 2001. A novel method to identify protein kinase substrates: eEF2 kinase is phosphorylated and inhibited by SAPK4/p38delta. EMBO J. **20**:4360-4369.

27. **Kruiswijk, F., L. Yuniati, R. Magliozzi, T. Y. Low, R. Lim, R. Bolder, S. Mohammed, C. G. Proud, A. J. Heck, M. Pagano, and D. Guardavaccaro**. 2012. Coupled Activation and Degradation of eEF2K Regulates Protein Synthesis in Response to Genotoxic Stress. Sci. Signal. **5**:ra40.

28. **Laderoute, K. R., K. Amin, J. M. Calaoagan, M. Knapp, T. Le, J. Orduna, M. Foretz, and B. Viollet**. 2006. 5'-AMP-activated protein kinase (AMPK) is induced by low-oxygen and glucose deprivation conditions found in solid-tumor microenvironments. Mol. Cell Biol. **26**:5336-5347.

29. **Lee, K., H. Zhang, D. Z. Qian, S. Rey, J. O. Liu, and G. L. Semenza**. 2009. Acriflavine inhibits HIF-1 dimerization, tumor growth, and vascularization. Proc. Natl. Acad. Sci. U. S. A **106**:17910-17915.

30. **Lehane, C., T. Guelzow, S. Zenker, A. Erxleben, C. I. Schwer, B. Heimrich, H. Buerkle, and M. Humar**. 2013. Carbimazole is an inhibitor of protein synthesis and protects from neuronal hypoxic damage in vitro. J. Pharmacol. Exp. Ther. **347**:781-793.

31. **Leprivier, G., M. Remke, B. Rotblat, A. Dubuc, A. R. Mateo, M. Kool, S. Agnihotri, A. El-Naggar, B. Yu, S. S. Prakash, B. Faubert, G. Bridon, C. E. Tognon, J. Mathers, R. Thomas, A. Li, A. Barokas, B. Kwok, M. Bowden, S. Smith, X. Wu, A. Korshunov, T. Hielscher, P. A. Northcott, J. D. Galpin, C. A. Ahern, Y. Wang, M. G. McCabe, V. P. Collins, R. G. Jones, M. Pollak, O. Delattre, M. E. Gleave, E. Jan, S. M. Pfister, C. G. Proud, W. B. Derry, M. D. Taylor, and P. H. Sorensen**. 2013. The eEF2 Kinase Confers Resistance to Nutrient Deprivation by Blocking Translation Elongation. Cell **153**:1064-1079.

32. **Liu, J. C., V. Voisin, S. Wang, D. Y. Wang, R. A. Jones, A. Datti, D. Uehling, R. Al-Awar, S. E. Egan, G. D. Bader, M. Tsao, T. W. Mak, and E. Zacksenhaus**. 2014. Combined deletion of Pten and p53 in mammary epithelium accelerates triple-negative breast cancer with dependency on eEF2K. EMBO Mol. Med. **6**:1542-1560.

33. **Loenarz, C., R. Sekirnik, A. Thalhammer, W. Ge, E. Spivakovsky, M. M. Mackeen, M. A. McDonough, M. E. Cockman, B. M. Kessler, P. J. Ratcliffe, A. Wolf, and C. J. Schofield**. 2014. Hydroxylation of the eukaryotic ribosomal decoding center affects translational accuracy. Proc. Natl. Acad. Sci. U. S. A **111**:4019-4024.

34. **Majmundar, A. J., W. J. Wong, and M. C. Simon**. 2010. Hypoxia-inducible factors and the response to hypoxic stress. Mol. Cell **40**:294-309.

35. **Middelbeek, J., K. Clark, H. Venselaar, M. A. Huynen, and F. N. van Leeuwen**. 2010. The alpha-kinase family: an exceptional branch on the protein kinase tree. Cell Mol. Life Sci. **67**:875-890.

36. **Moore, C. E., M. S. Regufe da, H. Mikolajek, and C. G. Proud**. 2014. A Conserved Loop in the Catalytic Domain of Eukaryotic Elongation Factor 2 Kinase Plays a Key Role in Its Substrate Specificity. Mol. Cell Biol. **34**:2294-2307.

37. **Pavur, K. S., A. N. Petrov, and A. G. Ryazanov**. 2000. Mapping the functional domains of elongation factor-2 kinase. Biochemistry **39**:12216-12224.

38. **Pigott, C. R., H. Mikolajek, C. E. Moore, S. J. Finn, C. W. Phippen, J. M. Werner, and C. G. Proud**. 2011. Insights into the regulation of eukaryotic elongation factor 2 kinase and the interplay between its domains. Biochem. J. **442**:105-118.

39. **Redpath, N. T., E. J. Foulstone, and C. G. Proud**. 1996. Regulation of translation elongation factor-2 by insulin via a rapamycin-sensitive signalling pathway. EMBO J. **15**:2291-2297.

40. **Redpath, N. T. and C. G. Proud**. 1993. Cyclic AMP-dependent protein kinase phosphorylates rabbit reticulocyte elongation factor-2 kinase and induces calcium-independent activity. Biochem. J. **293**:31-34.

41. **Robinson, A., S. Keely, J. Karhausen, M. E. Gerich, G. T. Furuta, and S. P. Colgan**. 2008. Mucosal protection by hypoxia-inducible factor prolyl hydroxylase inhibition. Gastroenterology **134**:145-155.

42. **Romero-Ruiz, A., L. Bautista, V. Navarro, A. Heras-Garvin, R. March-Diaz, A. Castellano, R. Gomez-Diaz, M. J. Castro, E. Berra, J. Lopez-Barneo, and A. Pascual**. 2012. Prolyl Hydroxylase-dependent Modulation of Eukaryotic Elongation Factor 2 Activity and Protein Translation under Acute Hypoxia. J. Biol. Chem. **287**:9651-9658.

43. **Ryazanov, A. G., B. B. Rudkin, and A. S. Spirin**. 1991. Regulation of protein synthesis at the elongation stage. New insights into the control of gene expression in eukaryotes. [Review]. FEBS Lett. **285**:170-175.

44. **Singleton, R. S., P. Liu-Yi, F. Formenti, W. Ge, R. Sekirnik, R. Fischer, J. Adam, P. J. Pollard, A. Wolf, A. Thalhammer, C. Loenarz, E. Flashman, A. Yamamoto, M. L. Coleman, B. M. Kessler, P. Wappner, C. J. Schofield, P. J. Ratcliffe, and M. E. Cockman**. 2014. OGFOD1 catalyzes prolyl hydroxylation of RPS23 and is involved in translation control and stress granule formation. Proc. Natl. Acad. Sci. U. S. A **111**:4031-4036.

45. **Speicher, K. D., O. Kolbas, S. Harper, and D. W. Speicher**. 2000. Systematic analysis of peptide recoveries from in-gel digestions for protein identifications in proteome studies. J. Biomol. Tech. **11**:74-86.

46. **Terai, K., Y. Hiramoto, M. Masaki, S. Sugiyama, T. Kuroda, M. Hori, I. Kawase, and H. Hirota**. 2005. AMP-Activated Protein Kinase Protects Cardiomyocytes against Hypoxic Injury through Attenuation of Endoplasmic Reticulum Stress. Mol. Cell Biol. **25**:9554-9575.

47. **Tiainen, M., K. Vaahtomeri, A. Ylikorkala, and T. P. Makela**. 2002. Growth arrest by the LKB1 tumor suppressor: induction of p21(WAF1/CIP1). Hum. Mol. Genet. **11**:1497-1504.

48. **Uniacke, J., C. E. Holterman, G. Lachance, A. Franovic, M. D. Jacob, M. R. Fabian, J. Payette, M. Holcik, A. Pause, and S. Lee**. 2012. An oxygen-regulated switch in the protein synthesis machinery. Nature **486**:126-129.

49. **Wiseman, S. L., Y. Shimizu, C. Palfrey, and A. C. Nairn**. 2013. Proteasomal degradation of eukaryotic elongation factor-2 kinase (EF2K) is regulated by cAMP-PKA signaling and the SCFbetaTRCP ubiquitin E3 ligase. J. Biol. Chem. **288**:17803-17811.

50. **Wong, H. K., M. Fricker, A. Wyttenbach, A. Villunger, E. M. Michalak, A. Strasser, and A. M. Tolkovsky**. 2005. Mutually exclusive subsets of BH3-only proteins are activated by the p53 and c-Jun N-terminal kinase/c-Jun signaling pathways during cortical neuron apoptosis induced by arsenite. Mol. Cell Biol. **25**:8732-8747.

836 FIGURE LEGENDS:

837 **Fig. 1. Hypoxia or DMOG treatment induces phosphorylation of eEF2 in diverse cell**
838 **types**. (A-F) The indicated cells were subjected to hypoxia or treated with DMOG (1 mM)
839 for the indicated times. Cell lysates were subjected to western blot analysis using the
840 indicated antibodies. The graph in (A) shows quantitation of data from multiple
841 experiments, data are given as mean ± SEM (control cells without hypoxia =1; n = 3). Data
842 were analysed using a one-way ANOVA. (G) HeLa cells were exposed to FG-4497 for 6 h
843 at the concentrations indicated in the figure. Cell lysates were subjected to western blot
844 analysis using the indicated antibodies. The graph in (G) shows quantitation of data from
845 three experiments, data are given ± SEM (control cells without treatment =1). The positive
846 control for P-p38 MAP kinase is a sample from bone marrow-derived macrophages treated
847 with lipopolysaccharide.

848 **Fig. 2. eEF2K knockout strategy.** Generation of an eEF2K conditional knockout allele
849 (A) Murine eEF2K gene map and targeting vector. Rectangles represent the coding exons
850 of the eEF2K gene as well as the FRT sites and the neomycin resistance (Neo) cassette. The
851 targeting vector can be linearized with NotI (B) Genotyping of littermates.

852 **Fig. 3. Hypoxia induced eEF2K activation is independent of AMPK**. (A) HCT116 cells
853 were subjected to hypoxia (0.1% oxygen) for 16 h in the presence or absence of the AMPK
854 inhibitor MRT199665 (MRT). (B) WT or AMPK α1/α2 DKO MEFs were subjected to
855 hypoxia (0.1% oxygen) 16 h. Cell lysates were subjected to western blot analysis using the
856 indicated antibodies. (C) eEF2K mRNA levels were determined by RT-qPCR and

normalized to 18S rRNA. Data were analysed using an unpaired t-test. The inset shows western blot analysis of lysates of WT and AMPK-DKO MEFs; equal amounts of total protein were applied to the gel. The blots were developed using the indicated antibodies. (D) A549 cells were cultured in the presence or absence of 1 mM IPTG for 5 days to induce the knockdown of eEF2K. Cells were then treated with DMOG (1 mM) or AZD8055 (A8) (1 μM) for the times indicated in the figure. (E) Wild-type ($eEF2K^{+/+}$) or eEF2K knockout ($eEF2K^{-/-}$) MEFs were treated with DMOG (1 mM), or with AZD8055 (A8) (1 μM), for the indicated times. '0' indicates samples from cells that had been pre-incubated with or without MRT199665 for 30 min.Samples from cells incubated for 8h without DMOG were also analysed. Lysates were analysed by immunoblots as indicated. (F) HCT116 cells were treated with DMOG (1 mM) with/without the AMPK inhibitor MRT199665 for the times indicated. Cell lysates were subjected to western blot analysis using the indicated antibodies. ACC, acetyl-CoA carboxylase. (G) HCT116 cells were treated with DMOG (1 mM) or AZD8055 (1 μM) for the times indicated in the figure. Cell lysates were subjected to western blot analysis using the indicated antibodies.

Fig. 4. Hypoxia or DMOG induce eEF2 phosphorylation independently of changes in mTORC1 signaling. (A) $TSC2^{+/+}$ or $TSC2^{-/-}$ MEFs were treated with DMOG (1 mM) for the indicated times or (B) subjected to hypoxia (0.1%) for 16 h. Equal amounts of cell lysates were analysed by SDS-PAGE/western blot using the indicated antibodies. The graph in (A) shows quantitation of data from multiple experiments, data are given as mean ± SEM (control cells without DMOG =1; n = 3). Data were analysed using an unpaired t-test. In (C) and (D), $TSC2^{+/+}$ and $TSC2^{-/-}$ MEFs were treated with 1 mM DMOG for 16 h.

EEF2K and *GLUT1* mRNA levels were determined by RT-qPCR respectively following DMOG treatment. Data are shown as mean ± SEM, n = 3 normalized to 18S rRNA. Data were analysed using a two-way ANOVA. In (E), where indicated, cells were treated with DMOG (1 mM) in the presence or absence of acriflavine (ACF; 5 μM). Equal amounts of cell lysate were analysed by SDS-PAGE/western blot using the indicated antibodies.

Fig. 5. Hypoxia or DMOG-treatment enhance the intrinsic activity of eEF2K. (A-D), the indicated cells were treated with DMOG or subjected to hypoxia (16h) and eEF2K activity was determined either in whole cell lysates (WCL; A,C) or after IP of FLAG-tagged eEF2K (B; in the presence or absence of Ca^{2+} as indicated). The immunoblot below shows total eEF2K levels in lysates from control or DMOG-treated cells. (C) MEFs were treated for 6 h with DMOG and cell lysates were subjected to western blot analysis using the indicated antibodies. (D) eEF2K activity was determined in whole cell lysates or, after IP, in the presence or absence of CaM. Shown are phosphorimages of the corresponding SDS gels.

Fig. 6. eEF2K is subject to hydroxylation on a highly-conserved proline residue. (A) (Top) Schematic depiction of the overall layout of eEF2K; the sequence of the CaM-binding site and adjacent residues is shown; Pro98 is indicated in red. (Bottom) sequences of the identified CaM-binding site in eEF2K proteins from the indicated species. Positions of Pro98 (bold, capital) and Trp99 (capital) are indicated. (B) A predicted mass spectrum plotted using the m/z values shown in Table 2 showing two potential sites for proline hydroxylation. (C) A representative MS/MS spectrum shows fragmentation of the HMPDPWAEFHLEDIATER peptide. A mass identical to a hydroxyproline-containing

fragment is observed, representing the HM(OH)PDP(OH)WAEFHLEDIATER peptide. A +32 Da mass shift is observed in the peptide from eEF2K under normoxic conditions; m/z = 2224.8 compared to the mass predicted from the sequence 2192.35. The spectrum shows the y ion series appearing at y14 m/z = 865.4 (2+) and y16 *m/z* 971.5 (+2) which assigns hydroxylation unambiguously to proline 98. The pertinent peaks are indicated (arrows).

Fig. 7. Hydroxylation on Proline-98 limits eEF2K activity. (A) HEK293 cells were transfected with a vector encoding FLAG-tagged eEF2K and, where shown, treated with DMOG (1 mM) for the entire period from transfection to lysis (20 h). Cells were lysed in extraction buffer containing CHAPs with calcium to maintain the CaM-eEF2K interaction. Cell lysates were assayed with or without CaM for 10 min using eEF2 as substrate. Data are phosphorimages of the corresponding SDS gels. Total eEF2K levels (WCL) were analysed by western blotting using anti-FLAG. (B-D) FLAG-tagged wild-type eEF2K or the [P96A] or [P98A] mutants were expressed in HEK293 cells which were subsequently treated with DMOG (6 h, 1 mM) where indicated. Immunoblot (IB) analyses using anti-FLAG (left side; also anti-tubulin) or anti-eEF2K, from lysates of cells ectopically expressing FLAG-eEF2K or non-transfected cells (endogenous eEF2K). In (C,D), (FLAG)-eEF2K activity was determined against eEF2 ± added calmodulin; in (D), data for assays conducted without added CaM; mean ±SEM, n=3. (E) FLAG-tagged wild-type eEF2K or the [P98A] mutant were expressed in HEK293 cells which were subsequently treated with DMOG (6 h, 1 mM) where indicated. Cells were lysed in extraction buffer containing

CHAPs and calcium to maintain the CaM-eEF2K interaction. Cell lysates were assayed with or without calcium and CaM for 10 min using eEF2 as substrate.

Fig. 8. Effect of hydroxylation of Pro98 on binding to CaM and of selected mutations at this position on eEF2K activity. (A,B) Isothermal calorimetry experiments were performed as described in the Experimental section using (A) unmodified peptide and (B) peptide hydroxylated on Pro98. The top graphs represent the original titration curve and bottom graphs show the resulting binding isotherm. (C) DMOG treatment of cells does not significantly the copurification of CaM and eEF2K. HEK 293 cells were transfected with a vector encoding FLAG-eEF2K. They were then maintained for 48 h in the presence or absence of 1mM DMOG from the point of transfection. Cells were lysed, and immunoprecipitations were carried out in a modified extraction buffer containing 1 mM $CaCl_2$ to maintain eEF2K-CaM interactions as described in Materials and Methods. The FLAG-tagged eEF2 kinase was immunoprecipitated from 200 µg of lysate protein using immobilized FLAG antibody and then subjected to SDS-PAGE followed by Western blotting for total eEF2 kinase or bound CaM. Blots for each protein are from non-adjacent lanes of the same gel. (D) The abilities of eEF2K and the indicated mutants to bind CaM were tested by affinity chromatography using CaM-Sepharose, using wild-type (WT) or the W99A, W99L or D97A mutants of bacterially-expressed eEF2K from which the GST tag had been removed by PreScission protease cleavage, as described in the Experimental section. Assays were conducted in the presence of CaCl. 1µg of cleaved WT eEF2K and mutant proteins were used in the pull-down with CaM resin and samples of the proteins

Molecular and Cellular Biology

(0.1µg) were run to display equal input levels. Samples were analysed by immunoblots using anti-eEF2K antibodies; the migration positions of GST-eEF2K and cleaved eEF2K are shown. (E) Activity of wild-type recombinant eEF2K or indicated mutants towards the MH1 peptide. Data are shown as mean ± SEM; n = 3. ***, $P < 0.001$ ****, $P < 0.0001$. *P* values were obtained using a two-way ANOVA compared with WT followed by Bonferroni post-tests. (F) Activity of wild-type or eEF2K[W99A] against eEF2. The upper part is a phosphorimage of the Coomassie-stained gel shown below.

Fig. 9. Time course for the synthesis of new eEF2K molecules. HEK293 cells were transfected with a vector encoding FLAG-eEF2K; 24 h later, cells were treated with cycloheximide (10 µg/mL) for 16 h, followed by release into cycloheximide-free medium for the indicated times. Cell extracts were prepared and run on SDS-PAGE, followed by Western blot using anti–FLAG and anti–tubulin antibodies.

Fig. 10. Loss of eEF2K compromises the ability of primary neuronal cells to withstand hypoxia. (A,B) primary neuronal cultures from control or eEF2K-knockout mice were maintained in culture for 7 days and then subjected to hypoxia (0.1% O_2, 20 h). ATP levels were measured using a CellTiter-Glo® Luminescent Cell Viability kit (A) or western blots performed for the indicated proteins (B). The graph in (B) shows the levels of cleaved PARP (n = 3, ±SEM; level of cleaved PARP in wild-type cells subjected to hypoxia is set at 1). Data were analysed using a two-way ANOVA. (C) $TSC2^{-/-}$ MEFS were treated with

DMOG (1 mM), rapamycin (200 nM) or cycloheximide (10 µg/ml) for 6 h and lysed. Samples were analysed by immunoblots using the indicated antibodies. (D) $TSC2^{-/-}$ MEFS were treated with DMOG (1 mM) (6 h) and then incubated with ^{35}S-methionine/cysteine (for the final 30 min). Samples were processed to measure incorporation of radiolabel into protein; data are shown ±SEM (n=3). Data were analysed using an unpaired t-test.

Moore Fig. 1

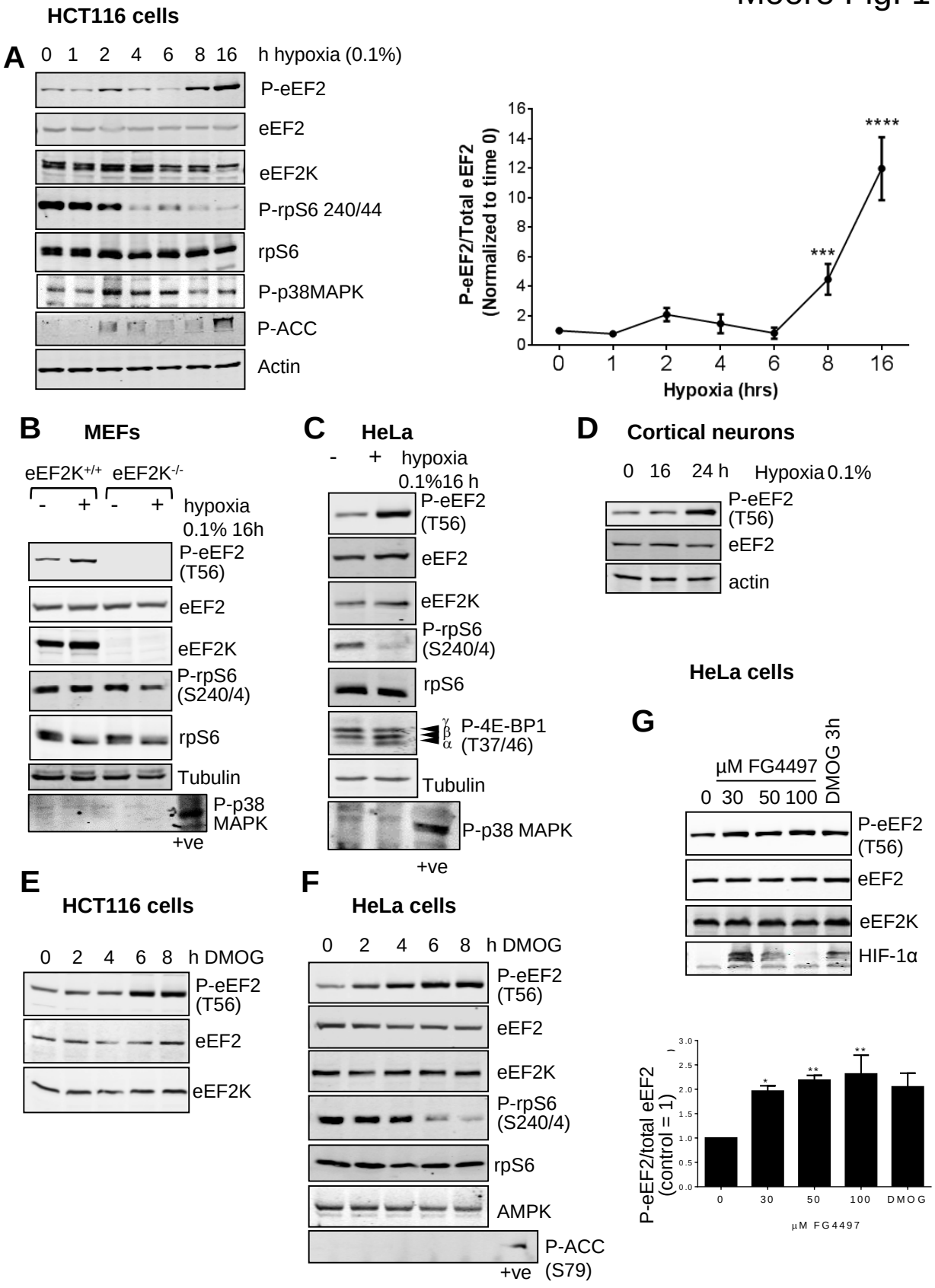

Moore Fig. 2

A

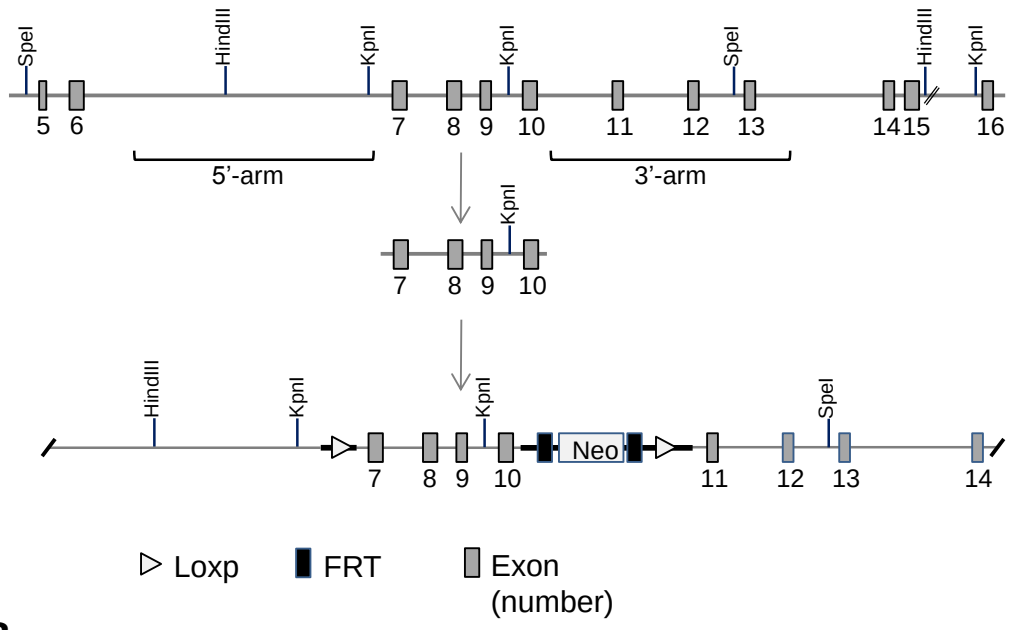

B

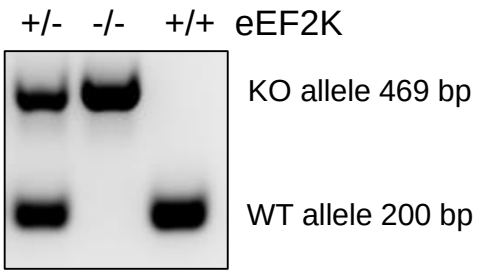

Moore Fig. 3

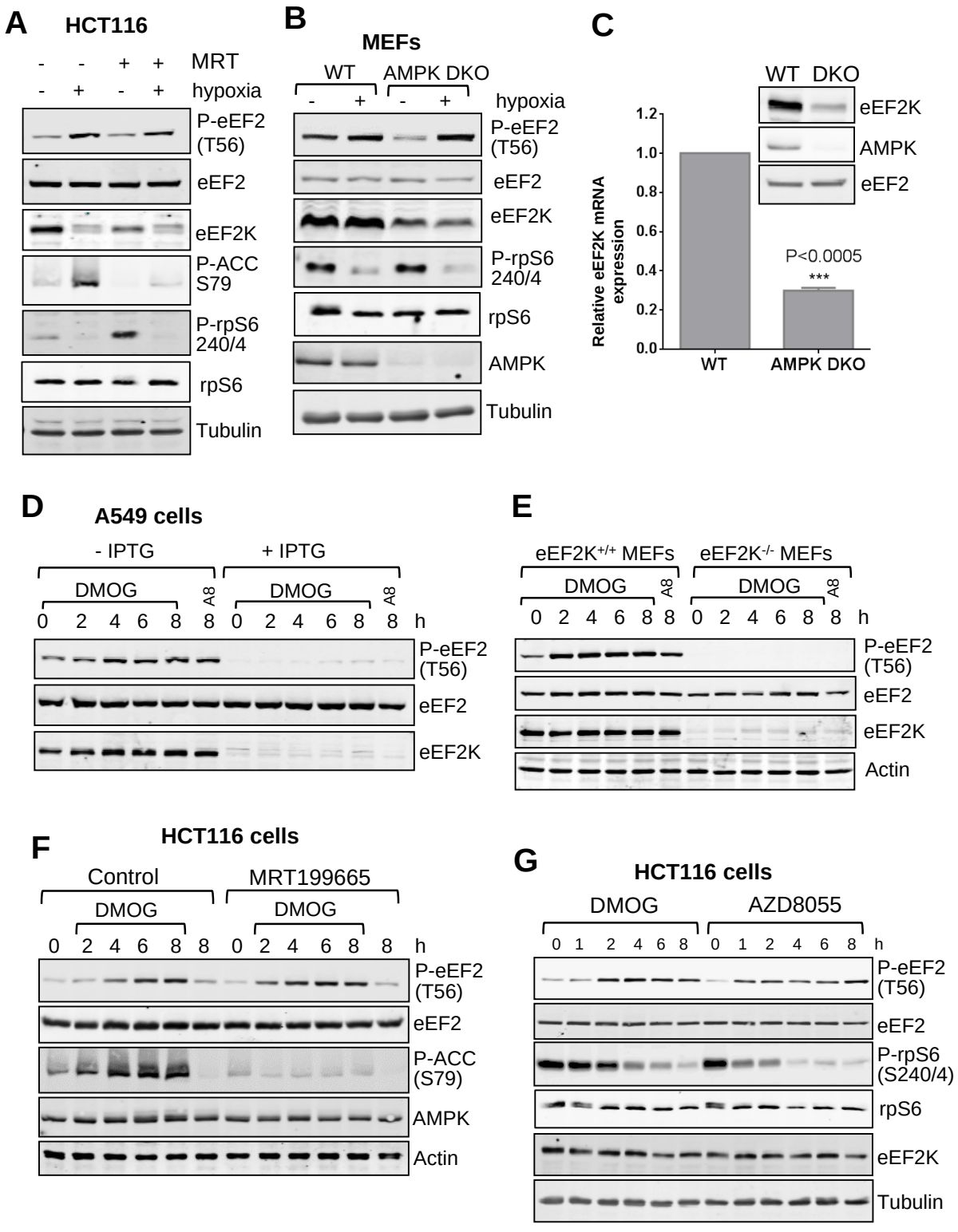

Moore Fig. 4

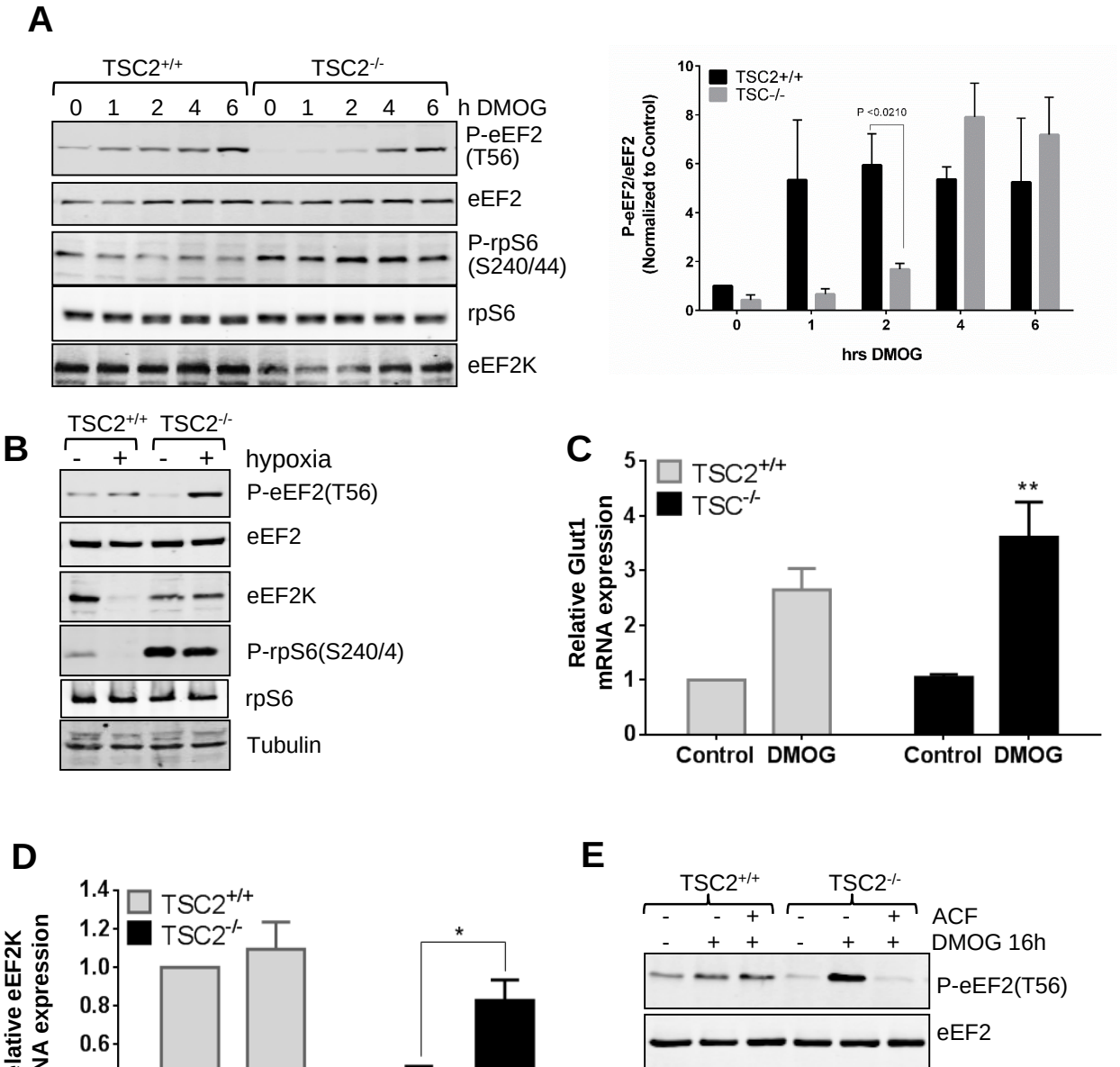

Moore Fig. 5

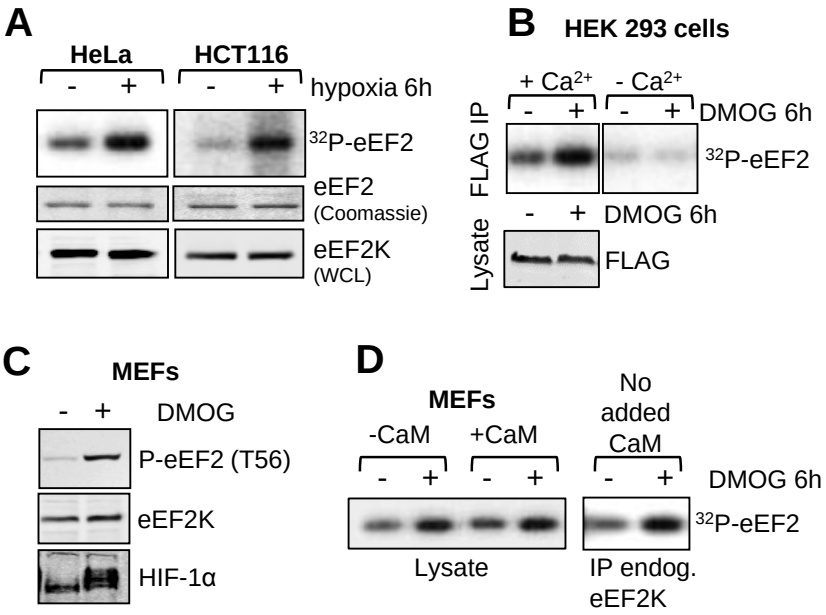

Moore Fig. 6

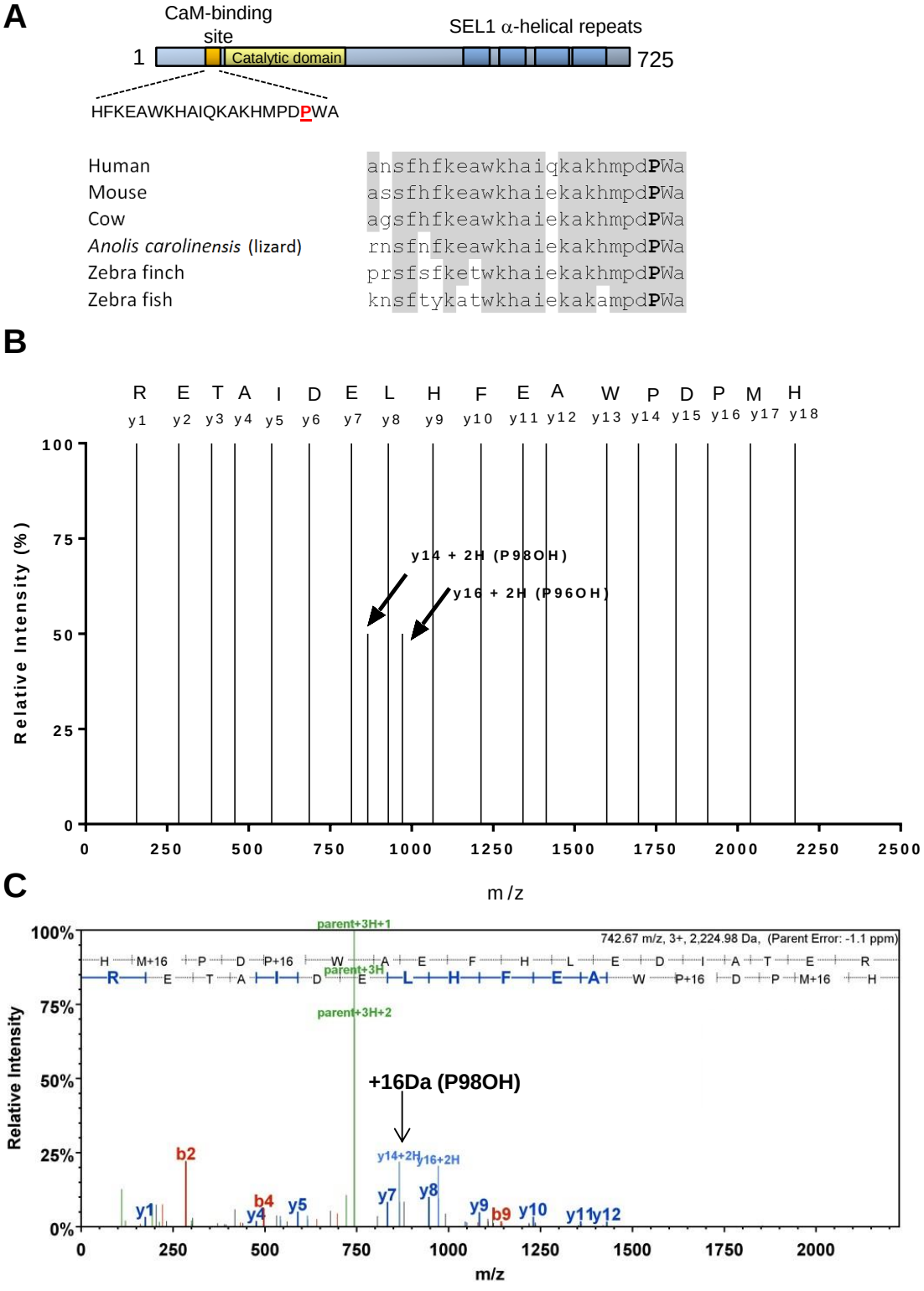

Moore Fig. 7

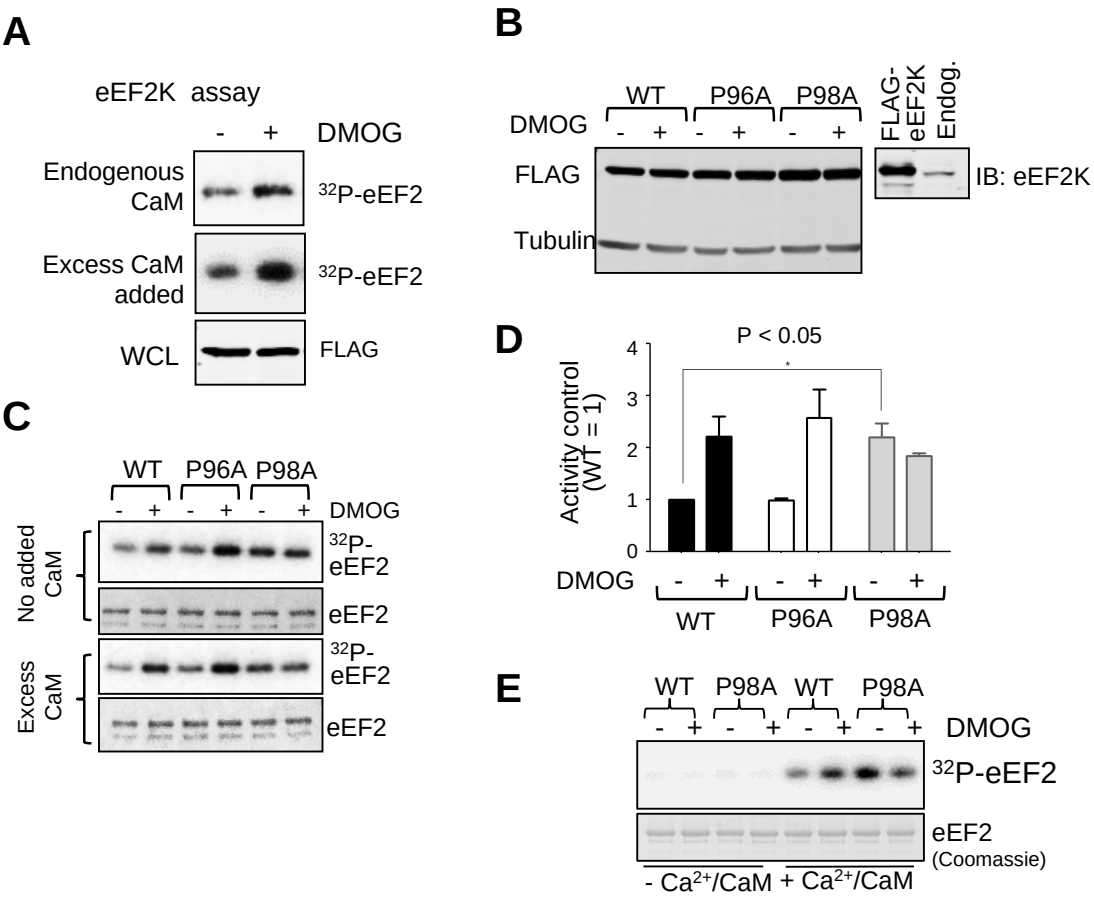

Moore Fig. 8

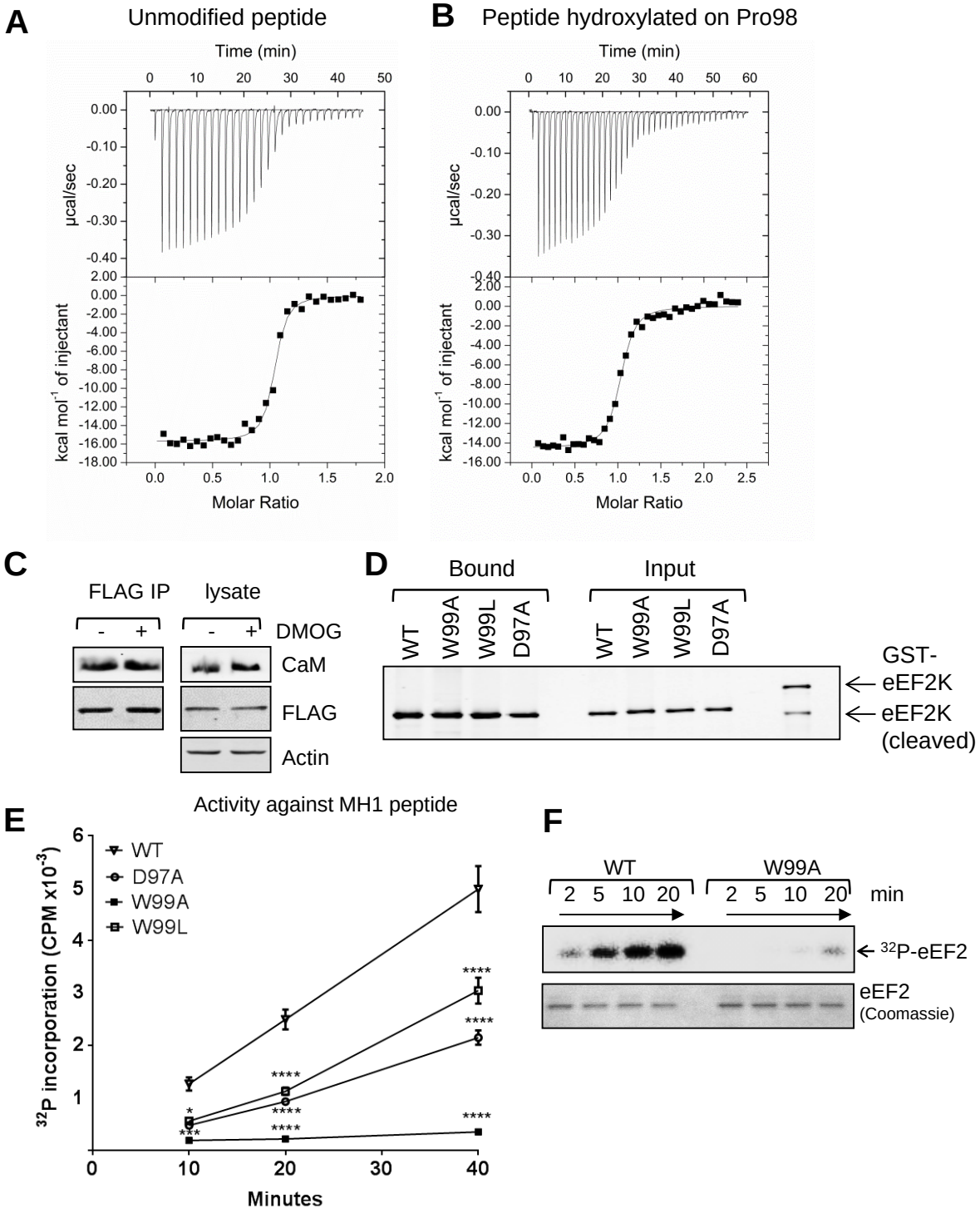

Moore Fig. 9

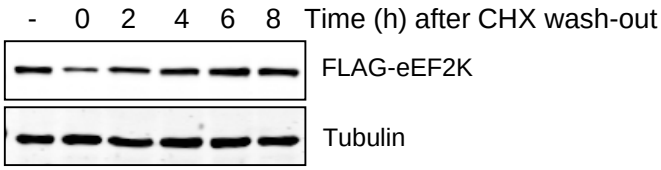

Moore Fig. 10

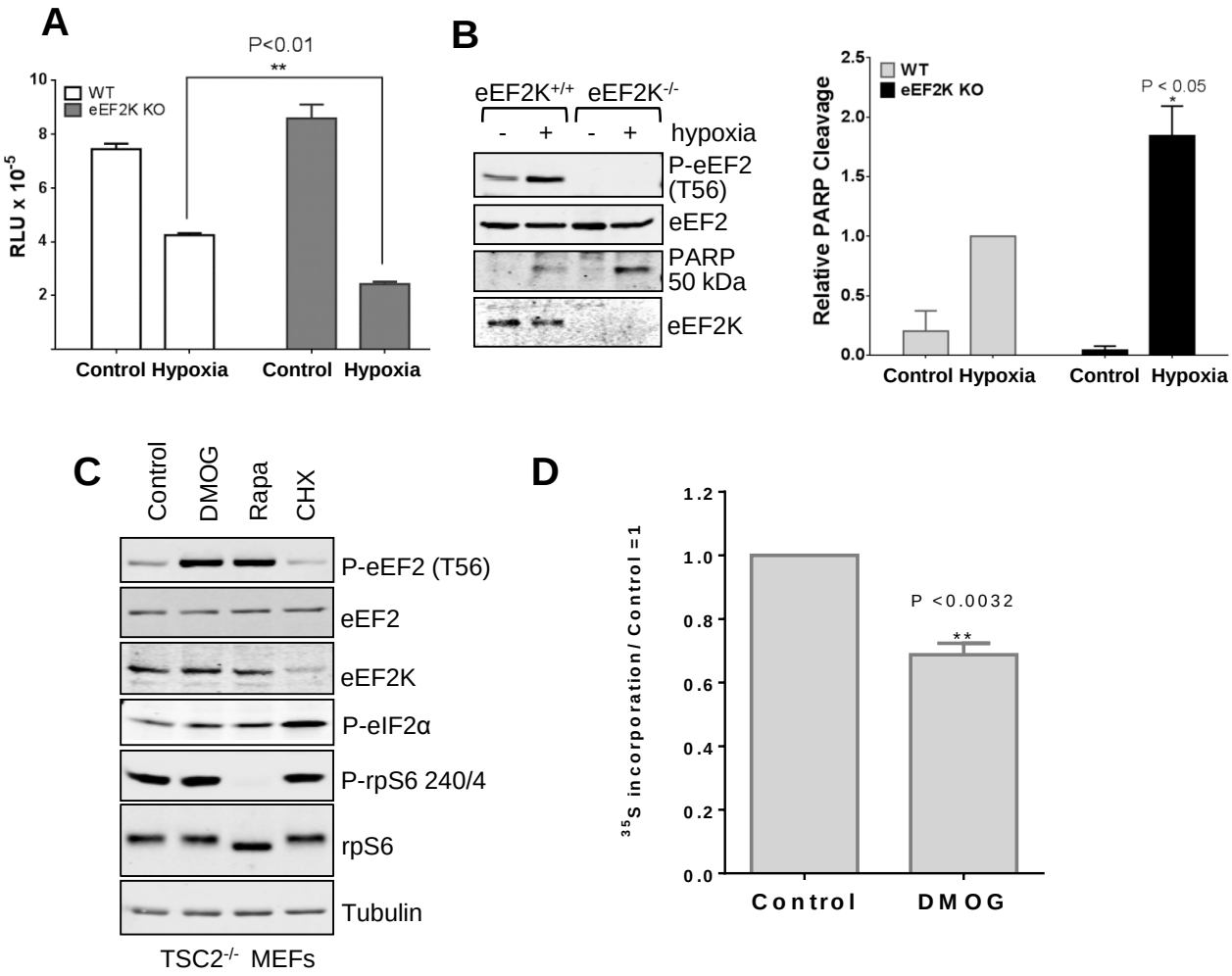

Table 1. m/z values for ions derived from the HMPDPWAEFHLEDIATER peptide.
(A) B- and y-ions for the above peptide from eEF2K from normoxic cells (hydroxyproline 98 is highlighted).
(B) Table of amino acid residue masses for the HMPDPWAEFHLEDIATER peptide, to assist with interpretation of the b- and y-ion series. Doubly-charged ions are indicated by, e.g., B + 2H.

(A)

B	B ions	B + 2H	Amino acid	Y ions	Y + 2H	Y
1	138.1	69.5	H	2226	1113.5	18
2	285.1	143.1	M + 16	2088.9	1045	17
3	382.2	191.6	P	1941.9	971.5	16
4	497.2	249.1	D	1844.8	922.9	15
5	610.2	305.6	P +16	1729.8	865.4	14
6	796.3	398.7	W	1616.8	808.9	13
7	867.3	434.2	A	1430.7	715.8	12
8	996.4	498.7	E	1359.7	680.3	11
9	1143.5	572.2	F	1230.6	615.8	10
10	1280.5	640.8	H	1083.5	542.3	9
11	1393.6	697.3	L	946.5	473.7	8
12	1522.6	761.8	E	833.4	417.2	7
13	1637.7	819.3	D	704.4	352.7	6
14	1750.8	875.9	I	589.3	295.2	5
15	1821.8	911.4	A	476.2	238.6	4
16	1922.8	961.9	T	405.2	203.1	3
17	2051.9	1026.4	E	304.2	152.6	2
18	2260	1113.5	R	175.1	88.1	1

(B)

b	b Ions	Amino acid	Mass	y Ions	y
1	137.1412	H	137.1412	2176.397	18
2	268.3398	M	131.1986	2039.256	17
3	365.4565	P	97.1167	1908.058	16
4	480.5451	D	115.0886	1810.941	15
5	577.6618	P	97.1167	1695.852	14
6	763.8751	W	186.2133	1598.736	13
7	834.9539	A	71.0788	1412.522	12
8	964.0694	E	129.1155	1341.443	11
9	1111.246	F	147.1766	1212.328	10
10	1248.3872	H	137.1412	1065.151	9
11	1361.5467	L	113.1595	928.0101	8
12	1490.6622	E	129.1155	814.8506	7
13	1605.7508	D	115.0886	685.7351	6
14	1718.9103	I	113.1595	570.6465	5
15	1789.9891	A	71.0788	457.487	4
16	1891.0942	T	101.1051	386.4082	3
17	2020.2097	E	129.1155	285.3031	2
18	2176.3973	R	156.1876	156.1876	1

Table 2. The sequence adjacent to the CaM-binding region, which contains the hydroxylated residue, Pro98, in eEF2K is highly conserved.

Residues shaded in grey are conserved between all vertebrate eEF2K sequences shown, and in some cases in eEF2K from nematodes. The first tryptophan is essential for binding of eEF2K to CaM (Diggle et al., 1999). Residues shown white on a black background are completely conserved in all species; the proline within this sequence corresponds to Pro98 of human eEF2K.

Mammals	
Homo sapiens	KEAWKHAIEKAKQ-MPDPWAEFHLEDIA
Pan troglodytes	KEAWKHAIQKAKQ-MPDPWAEFHLEDIA
Callithrix jacchus	KEAWKHAIEKAKQ-MPDPWAEFHLEDIA
Mus musculus	KEAWKHAIEKAKQ-MPDPWAEFHLEDIA
Cricetulus griseus	KEAWKHAIQKAKQ-MPDPWAEFHLEDIA
Oryctolagus cuniculus	KEAWKHAIEKAKQ-MPDPWAEFHLEDIA
Bos taurus	KEAWKHAIEKAKQ-MPDPWAEFHLEDVA
Tursiops truncates	KEAWKHAIEKAKQ-MPDPWAEFHLEDVA
Equus caballus	KEAWKHAIEKAKQ-MPDPWAEFHLEDIA
Loxodonta africana	KEAWKHAIEKAKQ-MPDPWAEFHLEDIA
Heterocephalus glaber	KEAWKHAIQKAKQ-MPDPWAEFHLEDIA
Felis catus	KEAWKHAIEKAKQ-MPDPWAEFHLEDIA
Dasypus novemcinctus	KEAWKHAIEKAKQ-MPDPWAEFHLEDIA
Sarcophilus harrisii	QETWKHAIEKAKQ-MPDPWAEFHLEDIE
Birds	
Gallus gallus	RETWKHAIEKAKQ-MPDPWAEFHLEDIE
Anas platyrhynchos	KETWKHAIEKAKQ-MPDPWAEFHLEDIE
Meleagris gallopavo	KETWKHAIEKAKQ-MPDPWAEFHLEDIE
Fish	
Maylandia zebra	RATWLHAIEKAKA-MPDPWAQFHLEEIA
Danio rerio	KATWKHAIEKAKA-MPDPWAEFHLEEME
Reptile	
Anolis carolinensis	KEAWKHAIEKAKQ-MPDPWAEFHLEEIE
Amphibian	
Xenopus tropicalis	KEAWKHAIQKAKQ-MPDPWAEFHLEDIE
Nematodes	
C. elegans	METWRKAARRARTNYIDPWDEFNIHEY
C. briggsae	METWRRAARRARSNYVDPWDEFNIHEY

Table 3. Isothermal titration calorimetry data for the interaction of Ca^{2+}/CaM with eEF2K-based peptides

Peptide	*K_d (nM)*	*ΔH (kcal/ mol)*	*ΔS at 298K (cal/mol)*	*-TΔS (kcal/ mol)*	*ΔG (kcal/ mol)*	*N*	*Number of expts*
eEF2K 78-100	66 ± 9.38	-15.2 ± 0.70	-18.4	-5.49	-9.76	0.99 ± 0.035	3
eEF2K 78-100 HO-Pro98	123 ± 2.64	-14.8 ± 0.18	-18.2	-5.43	-9.43	0.99 ± 0.007	3

Table of thermodynamic parameters obtained by fitting the ITC data to a single-state binding model (N = stoichiometry of the interaction determined in the experiment, K_d = dissociation constant, ΔH = change in enthalpy, ΔS =change in entropy, and ΔG = Gibb's free energy obtained by calculation of ΔG =ΔH - TΔS. Data are expressed as mean values ± standard deviation.